Studies in Relaxation Dynamics of Complex Systems: Exact Solution of Hysteresis in One Dimensional Anti-ferromagnetic Random Field Ising Model at Zero Temperature

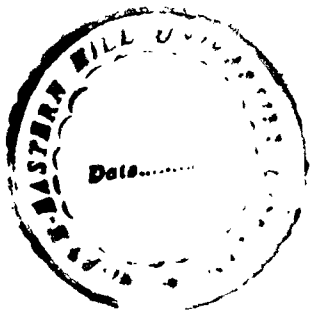

ABSTRACT

A THESIS SUBMITTED IN
FULFILMENT OF THE REQUIREMENT FOR
THE DEGREE OF

DOCTOR OF PHILOSOPHY
IN
SCIENCE

BY

RATNADEEP ROY

TO

DEPARTMENT OF PHYSICS
NORTH-EASTERN HILL UNIVERSITY
SHILLONG - 793 022

Studies in Relaxation Dynamics in Complex Systems: Exact Solution of Hysteresis in One Dimensional Anti-ferromagnetic Random Field Ising Model At Zero Temperature

(Abstract)

This thesis is a first step towards an exact determination of the non-equilibrium response of an anti-ferromagnet with quenched disorder. As indicated in the thesis, much of the effort in solving Ising models with quenched disorder has been focused on ferromagnetic models. To the best of our knowledge, exact solution of hysteresis in an anti-ferromagnetic Ising model with quenched disorder has not been attempted so far, although the problem was posed and solved approximately a few years ago [8,9]. In view of this situation we decided to determine the hysteretic response of the anti-ferromagnetic random field Ising model (AFRFIM). We were forced to make further simplifications by necessity. We limited our effort to one dimensional AFRFIM, zero-temperature Glauber dynamics, and the case when the applied field is ramped up and down infinitely slowly. In spite of these simplifications, it proved difficult to find the solution of the model for a general, unbounded, continuous distribution of the random field at par with the solution of the ferromagnetic RFIM [1-7]. The reason lies in the qualitative difference between the zero-temperature dynamics with ferromagnetic interactions and that with anti-ferromagnetic interactions. The ferromagnetic case is abelian [3], i.e. if we start

with any stable configuration of Ising spins, and then increase the external field and allow the system to relax, the final stable configuration reached is same and independent of the order in which the unstable spins are flipped. Also, in the relaxation process no spin flips more than once. In the anti-ferromagnetic case, the order in which the unstable spins are relaxed is important, and a spin which has flipped up in increasing field may flip down again at a higher field.

In the first instance [10,11], we considered a bounded, rectangular distribution of the random field of width 2Δ, with $\Delta \leq |J|$, where $|J|$ is the magnitude of the nearest neighbour anti-ferromagnetic interaction. In this case, the numerical simulation of the model shows that the magnetization on the lower hysteresis loop takes the form of three ramps separated by two plateaus. The model and its numerical simulations are described in Chapter II. The analysis of the three ramps is presented in Chapters III, IV, and V. We could not immediately generalize our solution for small disorder $(\Delta \leq |J|)$ to the case of large disorder $(\Delta \geq |J|)$, and to unbounded distributions of the random field. Some progress has been made in this direction,

but only recently. This is presented in Chapter VI. Finally Chapter VII contains a summary of our results and concluding remarks.

References

[1] P. Shukla, Physica A **233**, 235 (1996).

[2] D. Dhar, P. Shukla, and J. P. Sethna, J. Phys. A: Math. Gen. **30**, 5259 (1997).

[3] S. Sabhapandit, P. Shukla, and D. Dhar, J. Stat. Phys. **98**, 103 (2000).

[4] P. Shukla, Phys. Rev. **E 62**, 4725 (2000).

[5] P. Shukla, Phys. Rev. **E63**, 027102 (2001).

[6] P. Shukla, Ind. J. Phys. **76A** (1), 51 (2002).

[7] S. Sabhapandit, D. Dhar, and P. Shukla, to appear in Phys. Rev. Lett. (2002).

[8] P. Shukla, Physica A **233**, 242 (1996).

[9] P. Shukla, Ind. J. Phys. **72A** (5), 439 (1998).

[10] P. Shukla, R. Roy, and Emilia Ray, Physica A **275**, 380 (2000).

[11] P. Shukla, R. Roy, and Emilia Ray, Physica A **276**, 365 (2000).

Studies in Relaxation Dynamics of Complex Systems: Exact Solution of Hysteresis in One Dimensional Anti-ferromagnetic Random Field Ising Model at Zero Temperature

A THESIS SUBMITTED IN
FULFILMENT OF THE REQUIREMENT FOR
THE DEGREE OF

DOCTOR OF PHILOSOPHY
IN
SCIENCE

BY

RATNADEEP ROY

TO

DEPARTMENT OF PHYSICS
NORTH-EASTERN HILL UNIVERSITY
SHILLONG - 793 022

The North Eastern Hill University
April 2002

I Ratnadeep Roy , hereby declare that the subject matter of this thesis is the record of work done by me, that the contents of this thesis did not form basis of the award of any previous degree to me or to the best of my knowledge to anybody else, and that the thesis has not been submitted by me for any research degree in any other University/Institute.

This is being submitted to the North Eastern Hill University for the degree of Doctor of Philosophy in Physics.

Ratnadeep Roy

(Ratnadeep Roy)

18.4.02

Prof. M. K. Parida

Head, Dept. of Physics

Prabodh Shukla
18/4/02

Prof. Prabodh Shukla

Supervisor

Dedicated to
"Dadu"

Acknowledgement

Keeping with tradition this page is for acknowledging the help from persons received during the completion of this work.

First and foremost I would like to thank my guide Prof. Prabodh Shukla who was instrumental in suggesting this problem and without whose help this work would not have seen the light of the day. I would also take the opportunity to thank him for being so patient with me in spite of my being "slow".

I would like to thank my teachers especially Mr. Debasish Choudhury who taught me to look beyond the equations while studying Physics. I would also like to thank Dr. T. K. Sinha and Dr. S. Aravamudan who always took keen interest in my work and who always gave me new insights into the problem.

I am also thankful to the staff of Physics Department especially the Librarians- Mr. L. Jarian and Mr. P. S. Nongsiej for all the help I received from them.

Assistance from a DST Research Project- "Relaxational Dynamics in a Complex Landscape" is gratefully acknowledged.

I would also thank my friends Rajesh and Sabyasachi who always egged me to complete the work and in whose company I felt reassured.

Thanks are also due to Mr. Ayon Bhattacharjee with whom I had some useful discussions.

My gratitude to Dr. Sudipta Dey and Dr. Sanghita Dutta who always stood by me in all my ups and downs during the completion of this work.

Lastly I would like to mention my Baba, Ma and Didi and especially my friend Bornali all of whom I can never thank enough for all that they have done for me.

Ratnadeep Roy

Place: Shillong

Date: 18 - 04 - 2002 (Ratnadeep Roy)

CONTENTS

		Page No.
I.	**Introduction**	
I.1	Importance of Exactly Solved Models	1
I.2	Non-Equilibrium Phenomena	4
I.3	Hysteresis	6
I.4	Analysis of Hysteresis Loops	8
I.5	Complexity	12
I.6	Quenched Disorder and Separation of Time Scales	16
I.7	Random Field Ising Model	20
I.8	Our Work	23
II.	**The Model and Simulations**	
II.1	Motivation	27
II.2	The Model	28
II.3	Simulations	29
III.	**Ramp-I**	
III.1	Introduction	33
III.2	Screening Pairs	34
III.3	Magnetization on Ramp- I	38
IV.	**Ramp-II**	
IV.1	Plateau-I	39
IV.2	Magnetization on Ramp-II	47

V. Ramp-III

V.1 Plateau-II 53

V.2 Magnetization on Ramp-III 58

V.3 Creation of New Singlets 61

V.4 Destruction of New Singlets 71

V.5 Hysteresis Loop 73

V.6 Discussion 75

VI. Large Disorder

VI.1 Introduction 78

VI.2 Screening Pairs 79

VI.3 Magnetization on Lower Hysteresis Loop 87

VII. Summary and Concluding Remarks 99

References 101

Bio-Data 107

CHAPTER– I

I. Introduction

I.1 Importance of Exactly Solved Models

Statistical mechanics has made great strides in recent decades. The behaviour of systems in equilibrium is now understood quite well including phase transitions. Simple but exactly solved models have played an important role in the development of equilibrium statistical mechanics. Ising model [1] is one of the simplest and perhaps the most extensively studied model of cooperative behaviour in an extended system. The model is defined on a d-dimensional lattice, with lattice points denoted by $i=1, 2, 3,...N$. We are interested in the thermodynamic limit $N \to \infty$. Each lattice point i is assigned a dynamical degree of freedom called an Ising spin S_i. An Ising spin is a binary variable. It can take the values 0 or 1, or any other set of two values depending on the context of the physical system. In modelling a magnetic system it is customary to assign the values +1 (up) or −1 (down) to S_i. The magnetization (per site) is simply the average orientation of the Ising spins, i.e.

$$m = \frac{1}{N}\sum_{i=1}^{N} S_i \qquad (I.1)$$

Nearest neighbour Ising spins are coupled to each other through an exchange interaction J. Thus an Ising model is characterized by the Hamiltonian

$$H = -J\sum_{nn} S_i S_j \qquad (I.2)$$

If $J > 0$ (ferromagnetic coupling), the interaction aligns nearest neighbour spins parallel to each other. This produces a long range ferromagnetic order in the system, and therefore a net magnetization. If the system is in thermal equilibrium with a heat bath at a temperature T, the thermal energy $k_B T$ acts to disrupt the long range order. We may expect long-range order to prevail at low temperatures, and disorder at high temperatures. There may be a phase transition from an ordered state to a disordered state at a critical temperature T_c given approximately by the equation $k_B T_c \approx zJ$, where z is the number of nearest neighbour of a site on a d-dimensional lattice, and k_B is the Boltzmann constant. The primary motivation in introducing the Ising model is to calculate T_c,

and the singularities in the thermodynamic functions at the critical point.

The Ising model is easily solved in one dimension. It was solved by Ising in 1925 [2]. Surprisingly, the result showed that the critical temperature T_c in one dimension is equal to zero. The absence of long-range order at any finite temperatures is a special feature of one dimensional models with short-range interactions. It is now understood in a broader context as a result of theorems due to Landau, Mermin, and Wagner [3, 4]. This is an illustration of how exact solutions of very simple models can bring out a result of more general validity, and deepen our understanding.

Going beyond the one dimensional case, the simplicity of the Ising model turns out to be rather deceptive. The solution of the model in two dimensions is quite difficult. It was solved by Onsager in 1944 [5]. The Onsager solutions still remains a classic piece of work in equilibrium statistical mechanics and a required reading for a serious student of the subject. The solution was also extended to the case of a vanishingly small applied field in two dimensions [6]. The two dimensional Ising model in a finite applied field, and the three

dimensional Ising model even in the absence of an applied field have not been solved exactly so far in spite of a great effort. However, extensive numerical studies of the three dimensional Ising model have been made, as also analytical studies based on perturbation theory (high temperature expansion) [7]. These studies have contributed greatly to the theoretical understanding of universality and scaling in critical phenomena [8-10].

I.2 Non – Equilibrium Phenomena

Following the success of equilibrium statistical mechanics, attention has turned increasingly to non-equilibrium phenomena. A basic difference between equilibrium and non-equilibrium phenomena is the role of relaxation dynamics in non-equilibrium phenomena. By relaxation, we mean a process by which a system lowers its free energy to attain thermal equilibrium with its surroundings. The equilibrium state is the state of lowest free energy of the system. The properties of a system in equilibrium are independent of the relaxation path taken by the system to reach equilibrium. This results in a great simplification in the formulation of equilibrium statistical mechanics. The relaxation dynamics of a

system does not enter its equilibrium statistical mechanics. The success of equilibrium statistical mechanics arises from the fact that a great variety of physical systems relax very fast on the time scale of experimental observation. If the relaxation is slow or punctuated, we must take into account the relaxation dynamics of the system to understand its behaviour. This brings us to the subject of non-equilibrium statistical mechanics.

Non-equilibrium phenomena are generally as diverse as the systems exhibiting them. A first step towards their understanding would be to identify features that may have a weak universality going beyond the microscopic details of the system. Reasonable progress has been made in this direction. It has created several smaller fields of study which are better known by the key words such as coarsening , diffusion-limited-aggregation , viscous fingering [11-13], spinglasses [14-18], neural networks [19-25], persistence [26,27] etc. These keywords represent different aspects of weakly universal features seen in a wide variety of non-equilibrium phenomena. Simple models which provide an interesting caricature of these

phenomena have been identified, studied numerically as well as analytically, and compared with experiments.

I.3 Hysteresis

Hysteresis is a common feature of non-equilibrium phenomena. Webster's New Collegiate dictionary tells us:

Hys-ter-e-sis: n [NL, fr. Gk *hysteresis* shortcoming, fr. *hysterein* to be late, fall short, fr. *hysteros* later] a retardation of the effect when the forces acting upon a body are changed (as if from viscosity or internal friction); esp.: a lagging in the values of resulting magnetization in a magnetic material (as iron) due to a changing magnetizing force. - **hys-ter-et-ic** adj.

It is clear that hysteresis represents history dependence of physical systems. The term is most commonly applied to magnetic systems: as the external field associated with the microphone is turned off, little magnetic domains created by the recorded voice in the tape do not return to their original configuration (by design, otherwise our record of the music would disappear !). Generally any system which is capable of several configurations of equilibria for given external conditions exhibits hysteresis. Hysteresis in a

magnetic system is also the focus of this thesis. For the sake of completeness, we recall what is meant by hysteresis in a magnetic system. We take a magnet and drive it by a smoothly varying cyclic field of frequency ω. For simplicity we take the starting value of applied field to be very large and negative. Let us represent the applied field by the equation $h(t) = -h_o \cos \omega t$. Thus at the start of the hysteresis experiment, i.e. at time $t = 0$, the applied field is equal to $-h_o$. We assume that this initial value is large enough to saturate the magnetization in the downward direction, i.e. $m = -1$, at t = 0. As the applied field goes through a cycle the magnetization traces out a loop in the m-h plane. There are two values of magnetization for each applied field; the magnetization in increasing field being smaller than the magnetization in decreasing field. This indicates that we are observing a non-equilibrium effect where the response of the system lags behind the applied field. It may be expected that if the field is varied infinitely slowly, i.e. in the limit $\omega \to 0$, the system may be better able to keep pace with the applied field, and the hysteresis may disappear. This expectation is not always borne out by experiments and we shall say more on it later.

Suffice it to say here, that the existence of a loop even as $\omega \to 0$ is puzzling. In thermodynamic equilibrium, the system cannot exist in two distinct states except at a phase transition point. The hysteresis loop seems to indicate that the system has two thermodynamic states which are both stable at experimental time scales. This is a classic example of the conflicts between the predictions of classical equilibrium thermodynamics and empirical data that have existed since 19^{th} century.

In experiments the hysteresis loops corresponding to subsequent cycles of the applied field often do not overlap each other perfectly. Rather, with each subsequent cycle of the applied field, the hysteresis loop shifts slightly and systematically. This is a complex phenomenon known as reptation [28]. We shall not go into it further in this thesis. We are concerned with simple hysteresis loops that connect the system between two states of oppositely saturated magnetization and which do not show reptation.

I.4 Analysis of Hysteresis Loops

Even the simple hysteresis loops mentioned above are difficult to obtain theoretically. Readers would appreciate that all hysteresis

loops encountered by them are (most probably) of an experimental origin. Efforts to understand hysteresis theoretically were pioneered by Raleigh [29] and Preisach [30]. In the present work we attempt to obtain hysteresis loops theoretically from simple exactly solved models.

It is worthwhile to ask if there are any characteristics of hysteresis loops whose significance might go beyond the specifics of the physical system. For example, we expect the area of the hysteresis loop to vanish as $\omega \to 0$, irrespective of the system. It is interesting to investigate if the area vanishes as a (universal?) power of ω, or how it might depend on the parameters h_0, ω and T characterizing the field and the system. This question has been investigated by several authors [31-33]. It has been suggested that in the limit $h_0, \omega \to 0$, the area scales as $(h_0\omega)^{1/2}$ .The limit $\omega \to 0$ means that the time period of the applied field tends to infinity. In other words, the time over which the applied field changes significantly is much larger than any other time scales in the experiment. The time period of the applied field is one of the characteristic time scales for the

system. The other time scale is determined by the thermal relaxation time of the system. In fact, in most systems, there is a whole spectrum of thermal relaxation times. In many practical cases the longest thermal relaxation time is larger than the time period of the applied field even if the field is cycled very slowly. In such cases the area of the hysteresis loop shows no indication of vanishing even if the applied field were to be cycled so slowly so as to take an entire life of an experimentalist to complete one cycle. The work presented in this thesis concerns these systems with infinitely slow thermal relaxation. We may conveniently set the temperature of the system equal to zero to model systems whose thermal relaxation is infinitely slow. The microscopic structure of magnetization loops in such systems can be broadly divided into two categories – (*i*) noisy, and (*ii*) smooth. The noisy structure is characteristic of ferromagnetic systems. Even though the applied field changes smoothly, the magnetization changes in sporadic jumps of irregular and unpredictable sizes. This is known as Barkhausen noise [34]. The Barkhausen noise shows an apparent power-law spectrum, and has been studied by several workers experimentally as well as

theoretically [35-39]. It is a paradigm of non-equilibrium response of systems that respond to slow and smooth applied forces by avalanches. Other systems in this category are sandpiles [40,41], earthquakes, and avalanches of snow on mountains. The second category of systems respond relatively smoothly (i.e. without avalanches) but infinitely slowly to smoothly changing forces. These systems are characteristic of anti-ferromagnetic interactions. The anti-ferromagnetic interactions ensure that an Ising spin that has flipped in response to a changing external field generally acts to stop its immediate neighbours from flipping. As we shall see below, there are exceptions to this rule. Occasionally a nearest neighbour may flip but the process does not continue beyond the nearest neighbour. There are no avalanches in this category of relaxation. Examples of physical systems showing this behaviour are amorphous anti-ferromagnets, glasses and spinglasses which continue in a metastable state for a long time and then transit to another by small localized events sans avalanches [42-44].

1.5 Complexity

Complexity is a topic of current research activity in a number of fields including statistical mechanics, computer science, mathematics and biology. Within such diverse groups it is not surprising that the term complexity is used with several shades of meaning. We shall not go into the various definitions of complexity, rather we will briefly mention what we understand by complexity in an intuitive way in the context of recent research, and then state more specifically in the context of this thesis. Generally we can describe an extended system at two levels: microscopic level and macroscopic level. Complexity refers to the richness of the description at the macroscopic level. Consider two examples: water (as a chemical) and an animal (a biological system). At the macroscopic level water is adequately described by stating the phase in which it exists e.g. is it liquid, vapour or ice? The phase in turn is specified uniquely by the temperature and pressure. There are critical points for water where two phases may coexist but generally it has a unique macrostate. On the contrary if our system is a biological system, its macroscopic description may be rich (an animal may run, sleep, eat, jump ...).

The variety of the macroscopic description is taken as an indication of complexity.

From this point of view, clearly all traditional physical systems are simple and apparently complexity is not relevant in the world of physics. However, in the last years the situation has changed: it has been found that there are many disordered physical systems for which the macroscopic description is quite rich. An example that is easy to visualize is a heteropolymer, i.e. a polymer composed of a sequence of many different functional units. Typical biological heteropolymers are proteins, DNA and RNA. Sometimes it happens that the same heteropolymer at low temperature folds in a unique way, but in other cases more than one folding is possible. If the heteropolymer may fold in many different ways, we can consider each folding as a different phase and such a system is a complex system [45, 46]. Other physical systems like spinglasses have similar properties; they have been carefully investigated and structure of different phases of the systems has been studied in details. It is striking that these systems have a rather interesting chaotic behaviour: a small change in the form of the system may completely

upset the macroscopic behaviour. This effect becomes more and more pronounced by increasing the size of the system. In the case of large systems the macroscopic behaviour is extremely difficult to predict because it is sensitive to a huge number of microscopic details.

This kind of difficulty is not without precedent in physics. Indeed the observation that for a given system the actual trajectory is extremely sensitive to the initial conditions (as billiard balls), destroyed the hope of computing the trajectory of a large system in a precise way (apart a few exceptions). However the birth of statistical mechanics is related to this difficulty; the unpredictability of the trajectory in a deterministic sense makes possible to obtain probabilistic predictions for the behaviour of the system for generic initial conditions. The main proposal of Boltzmann was to give up the possibility of predicting the evolution of the system for given initial conditions and to concentrate the attention on the study of the most likely evolution starting from generic initial conditions. In the same way we can give up the possibility of computing which are all the macroscopic descriptions of a particular complex system. Doing

so we gain the possibility of obtaining statistical predictions on its behaviour. The statistical predictions however are different from the ones of usual statistical mechanics. In usual statistical mechanics the system is nearly always in one given macrostate and we compute the probability distribution of several different microscopic realizations of the same macrostate. Here we predict the probability of having a given number of simultaneously available macrostates and the relations among the different macrostates. Other interesting quantities that can be computed are, for example the average time spent by a system in a given macrostate before jumping into another macrostate.

For a large class of systems, a generic choice of the system implies the existence of many macroscopic states. In other words if the system is chosen in a random way, the macroscopic behaviour is automatically very rich. We do not need to tune the parameters that control our system in order to have many different macroscopic states because this feature is present in the generic case. We can summarize the situation by saying that microscopic randomness generates complexity.

I.6 Quenched Disorder and Separation of Time Scales

Disorder is really unavoidable in any thermodynamic system. The reason is that any system must have a finite entropy at a non zero temperature. However, there may be instances of small disorder e.g. a tiny fraction of point defects in an otherwise perfect crystal, or a large disorder that is characteristic of liquids. This separation of disorder between small disorder and large disorder does not have a sharp dividing line, but the meaning is intuitively clear. Similarly, there is another classification of disorder into two categories: annealed and quenched. This classification is based on the relaxation dynamics of the system. Thermodynamic systems have several modes of relaxation. The number of modes maybe infinitely large, and each mode has a different rate of relaxation. If the disorder is able to relax well over experimental time scales, we call it annealed disorder. Annealed disorder is the kind of disorder seen in very slowly cooled liquids and metals. If the disorder is not able to relax itself over the time periods of experimental observation i.e. if it remains frozen for all practical purposes, we call it quenched disorder. Examples of quenched disorder are glasses, spinglasses,

and other amorphous solids. It is quenched disorder that gives rise to a large number of macrostates of the system and hence to complex behaviour.

Again, the dividing line between what can relax and what remains frozen is not very sharp. It depends on the period over which the system is observed. Suppose the time of observation is τ_0, and the time of relaxation (inverse of relaxation rate) is τ_r. Quenched disorder corresponds to the case, $\tau_r >> \tau_0$. Even in this case, there is small probability that the slowest relaxation modes may affect the system during observation. However, for theoretical convenience, we shall impose a strict separation of time scales in the analysis of the system. Relaxation processes which occur extremely slowly will be assumed not to occur at all. Consider for example a glass. There is natural separation of time scales in this example. The mean positions of atoms change extremely slowly, while the vibrations around the mean positions (phonons) are fast. Quenched disorder assumes that the mean positions do not change at all.

In quenched systems, a fraction of the degrees of freedom is assumed to remain strictly frozen during the life time of the system,

and the remaining degrees of freedom evolve in this frozen background. Due to the randomly frozen background in which the system has to evolve, its evolution depends strongly on the initial state i.e. the history of the system. If the time period of observation were truly infinite and all relaxation processes were allowed the evolution of the system will be punctuated by long-lived metastable states. Over practical time periods, the system explores only a limited phase space corresponding to the domain of a metastable state. Going back to our example of phonons in a glass, the glassy solid can only explore those phonon modes which are possible in the frozen configuration of the mean positions of atoms. It is not possible for the system to explore phonon modes belonging to a different realization of the distributions of mean positions of atoms.

Systems with quenched disorder have a large number of metastable states. As we discussed in the preceding section, the existence of several metastable states or macrostates give rise to complex behaviour. We shall take an extended system to be a complex system, if its free energy has a thermodynamically large number of local minima in the phase space of the system, and the

local minima are separated from each other by thermodynamically large energy barriers. Spinglasses are our paradigm of complex systems, and spinglass behaviour that of complexity. The local minima are the metastable states of the system. Large barriers mean that the metastable states have a very long lifetime. A system may stay in the same metastable state during the period of experimental observation. Thus the observed properties of the system should be obtained by averaging the system over the thermodynamic domain of a single metastable state, and then taking a second average over the distributions of local minima of free energy. The barriers separating various local minima are assumed to be random and mainly larger than thermal energy of the system. Experience with spinglasses and other random systems has shown that Ising models with quenched random interactions or quenched field on sites, produce a free energy landscape of the kind indicated above. However, models with quenched interactions have not been solved exactly even in the mean field approximation [17]. Random field Ising models (RFIM) are more amenable to exact solution. In the following, we describe the

nature of the work done on the RFIM so far before taking it up for further analysis in this thesis.

I.7 Random Field Ising Model

The random field Ising model (RFIM) has played an important role in understanding disordered systems. It first came into prominence around 1975, when Imry and Ma [47] argued that Ising magnets with quenched random field were capable of sustaining a long range order in two dimensions. It was an appealing argument, and a kind of clear statement which was lacking in the context of other prominent models of quenched disorder, e.g. the Sherrington-Kirkpatric (random bond) model of a spinglass. Thus several people were attracted to the study of the equilibrium statistical mechanics of the random field Ising model. Soon a controversy was generated. Dimensional reduction arguments based on field theoretic methods [48] showed that the lower critical dimensionality of RFIM was three rather than two as predicted by Imry and Ma. It took some years to resolve that the application of the dimensional reduction method in this context was unjustified because it necessarily assumed the existence of a unique solution of the field equations. It was shown

that the field equations for systems with quenched disorder have a large number of solutions (metastable states). Due to the presence of numerous metastable states in the system, the numerical simulations proved rather difficult and inconclusive, and the initial enthusiasm for the model faded in due course.

Some years later, interest in RFIM revived for the same reason it had faded earlier. Its richness in metastable states was a deterrent in the study of its equilibrium properties, but made a good model for the study of non-equilibrium phenomena in glassy and complex systems. These systems are characterised by extremely slow relaxation, and history dependent effects which arise from the presence of several metastable states in the system. Recently Sethna et al [49] used the RFIM to study hysteresis and other related phenomena such as the return point memory effect, and Barkhausen noise. Hysteresis is a kinetic phenomena, and therefore one needs to put in a dynamics in the model. Sethna et al employed the zero-temperature Glauber dynamics of Ising spins. It showed remarkable success in reproducing the observed features of hysteresis and other phenomena mentioned above. The success of the Sethna model is not

unreasonable. It forms a minimal model which takes into account the most important aspects of hysteresis. For complex systems of the kind indicated above, the zero-temperature dynamics is a reasonable approximation to the finite temperature dynamics on laboratory time scales. The thermal energies are anyway much smaller than barrier heights, therefore it is a reasonable approximation to assume that the thermal energy is zero. Although the dynamics is deterministic, there is a stochastic aspect to it coming from the randomness of the quenched field. The metastable states of the RFIM become fixed points (stable states) under the zero-temperature dynamics. This simplifies their numerical as well as analytic characterization. However, the model retains the key features of the original problem. There is a broad distribution of energy barriers between nearby stable states. When the system is driven by a smoothly increasing applied field, it jumps from a stable state to a nearby stable state of lower energy when the applied field crosses the barrier between the two states. As the barriers are random variables, the trajectory of the system is not smooth. On a microscopic scale, it consists of irregular jumps in the magnetization (Barkhausen noise).

For ferromagnetic systems, experiments show that there is a broad distribution of the size of the magnetization jumps. Averaged over the entire hysteresis loop, jump distribution shows power laws over several decades (usually three). This has led to suggestions that there is a self-organized criticality in the system. The Sethna model provides a framework for examining this question. Although it does not appear to support self-organized criticality in the system, but there is a "plain old critical point" on each half of the hysteresis loop. At this point, the magnetization jumps show true power laws. The critical region appears to be rather broad. Thus approximate power laws are expected over a wide sector of the hysteresis loop. The extensive study of the Sethna model is based on numerical simulations of the model, and its analysis in the mean field approximation. For ferromagnetic interactions, the zero temperature hysteresis loops, the distribution of sizes of the Barkhausen jumps, and minor hysteresis loops have been determined exactly in one dimension as well as on a Bethe Lattice [50-56].

I.8 Our Work

This thesis is a first step towards an exact determination of the

non-equilibrium response of an anti-ferromagnet with quenched disorder. As indicated in the previous section, much of the effort in solving Ising models with quenched disorder has been focused on ferromagnetic models. To the best of our knowledge, exact solution of hysteresis in an anti-ferromagnetic Ising model with quenched disorder has not been attempted so far, although the problem was posed and solved approximately a few years ago [57,58]. In view of this situation we decided to determine the hysteretic response of the anti-ferromagnetic random field Ising model (AFRFIM). We were forced to make further simplifications by necessity. We limited our effort to one dimensional AFRFIM, zero-temperature Glauber dynamics, and the case when the applied field is ramped up and down infinitely slowly. In spite of these simplifications, it proved difficult to find the solution of the model for a general, unbounded, continuous distribution of the random field at par with the solution of the ferromagnetic RFIM [50-56]. The reason lies in the qualitative difference between the zero-temperature dynamics with ferromagnetic interactions and that with anti-ferromagnetic interactions. The ferromagnetic case is abelian [52], i.e. if we start

with any stable configuration of Ising spins, and then increase the external field and allow the system to relax, the final stable configuration reached is same and independent of the order in which the unstable spins are flipped. Also, in the relaxation process no spin flips more than once. In the anti-ferromagnetic case, the order in which the unstable spins are relaxed is important, and a spin which has flipped up in increasing field may flip down again at a higher field.

In the first instance [59, 60], we considered a bounded, rectangular distribution of the random field of width 2Δ, with $\Delta \leq |J|$, where $|J|$ is the magnitude of the nearest neighbour anti-ferromagnetic interaction. In this case, the numerical simulation of the model shows that the magnetization on the lower hysteresis loop takes the form of three ramps separated by two plateaus. The model and its numerical simulations are described in Chapter II. The analysis of the three ramps is presented in Chapters III, IV, and V. We could not immediately generalize our solution for small disorder $(\Delta \leq |J|)$ to the case of large disorder $(\Delta \geq |J|)$, and to unbounded

distributions of the random field. Some progress has been made in this direction, but only recently. This is presented in Chapter VI. Finally Chapter VII contains a summary of our results and concluding remarks.

CHAPTER– II

II. The Model and Simulations

II.1 Motivation

Relaxation dynamics of random field Ising model (RFIM) at zero temperature provides a simple caricature of complex non-equilibrium phenomena. RFIM with ferromagnetic as well as anti-ferromagnetic interactions has been investigated in the context of two distinct classes of relaxational behaviour. The ferromagnetic RFIM shows relaxation by avalanches and has been applied to study hysteresis and Barkhausen jumps in magnetic materials[49-56]. The anti-ferromagnetic model does not support avalanches, and is more appropriate for the glassy kind of dynamics where relaxation may proceed by single localized events [42-44,61]. In spite of the simplicity of RFIM and its relaxational dynamics at zero temperature, exact solution of the model is difficult on account of its randomness. So far, analytic solution of the model has been obtained in one dimension and on a Bethe lattice for ferromagnetic interactions only. In the following, we present a solution of the non-equilibrium dynamics of the anti-ferromagnetic RFIM at zero temperature in one dimension in a limited range of the applied field. For simplicity, we limit ourselves to a bounded uniform distribution of the random field.

II.2 The Model

At each site of a one dimensional lattice, there is an Ising spin $s_i = \pm 1$, i=1, 2, 3,.....,n which interacts with its nearest neighbours through an anti-ferromagnetic interaction J (J<0). Each site has a quenched random field h_i drawn independently from a continuous bounded distribution,

$$p(h_i) = \frac{1}{2\Delta} \quad \text{if} \quad -\Delta \le h_i \le \Delta$$

$$= 0, \quad \text{otherwise} \qquad \text{(II.1)}$$

The entire system is placed in an externally applied uniform field h_a. The Hamiltonian of the system is given by

$$H = -J\sum_i s_i s_{i+1} - \sum_i h_i s_i - h_a \sum s_i \qquad \text{(II.2)}$$

We consider the hysteretic response of this system when the external field h_a is slowly increased from $-\infty$ to $+\infty$. We consider the dynamics to be the single-spin-flip Glauber dynamics at zero temperature, i.e. a spin is flipped only if it lowers the energy. We assume that if the spin-flip is allowed, it occurs with a rate Γ, which is much larger than the rate at which the magnetic field h_a is increased. Thus we assume that all flipable spins relax instantly, and the spin s_i always has the same sign as the net local field l_i at the site.

$$s_i = sign\ l_i = sign\ [J(s_i s_{i+1}) + h_i + h_a] \qquad \text{(II.3)}$$

The hysteretic response of the system to an applied field h_a is measured by the magnetization $m(h_a)$ per spin,

$$m(h_a) = \frac{1}{N}\sum_i s_i \qquad \text{(II.4)}$$

We start with $h_a = -\infty$, when $m = -1$, and increase h_a slowly to $h_a = +\infty$ when $m=1$. Our object is to calculate $m(h_a)$ for all values of h_a. The magnetization $m_R(h_a)$ on the return trajectory when h_a is slowly decreased from $h_a = +\infty$ to $h_a = -\infty$ can be obtained from $m(h_a)$ by a symmetry relation $m_R(h_a) = -m(-h_a)$. Therefore the knowledge of the magnetization curve on the lower half of the hysteresis loop suffices to determine the entire hysteresis loop, and we can limit ourselves to the calculation of $m(h_a)$ alone.

II.3 Simulations

It is instructive to look at a computer simulation of the model before proceeding to obtain it analytically. Figure (II.1) shows magnetization $m(h_a)$ in an increasing applied field h_a for an anti-ferromagnetic RFIM $(J = -1)$, obtained from a simulation of 10^3 spins averaged over 10^3 different realizations of the random field distribution of width $2\Delta = 1$. The magnetization $m(h_a)$ rises from -1 to $+1$ in three steps. We call

these steps as ramp-I ($h_a = -2|J| - \Delta$ to $h_a = -2|J| + \Delta$); ramp-II ($h_a = -\Delta$ to $h_a = +\Delta$); and ramp-III ($h_a = 2|J| - \Delta$ to $h_a = 2|J| + \Delta$). The ramps are connected to each other by two plateaus; plateau-I ($h_a = -2|J| + \Delta$ to $h_a = -\Delta$); and plateau-II ($h_a = +\Delta$ to $h_a = 2|J| - \Delta$). On the plateaus, the magnetization remains constant even though the applied field continues to increase. Plateaus occur for $\Delta \leq |J|$ (small disorder), and simulations suggest that magnetization on the plateaus is independent of Δ. Numerically, the magnetization on the plateaus is approximately $m^I = -0.135$ on plateau-I, and $m^{II} = 0.109$ on plateau-II.

The qualitative shape of $m(h_a)$ is easy to understand. Due to the anti-ferromagnetic interaction between nearest neighbours, spins with both neighbours down are the easiest to be turned up by an applied field increasing in the up direction. Such spins turn up on ramp-I. Next are the spins with one neighbour up and one down which turn up on ramp-II. Spins with both neighbours up require the largest applied field to turn up, and these turn up on ramp-III. On each ramp, the sequence in which the spins turn up is determined by the distribution of the quenched random field. Spins with large positive quenched field turn up before

spins with a lower quenched field. The quenched field lies in the range $-\Delta$ to $+\Delta$. Thus each ramp has a width 2Δ along the axis of the applied field.

When a spin turns up on ramp-I, its nearest neighbours are placed in a category that cannot turn up before ramp-II. Similarly when a spin turns up on ramp-II, its nearest neighbour which is down cannot turn up before ramp-III. This is essentially the reason for the absence of avalanches in the anti-ferromagnetic RFIM. Occasionally on ramp-II and ramp-III, a spin turning up can induce its nearest neighbour which is already up to turn down. We will discuss the situation on ramp-II in detail later, but suffice it to say here that this process too does not cause an avalanche. With anti-ferromagnetic interactions, spins turn up one at a time (no Barkhausen noise), and the calculation of $m(h_a)$ becomes essentially a matter of sorting quenched random fields in decreasing order on each ramp. The difficulty arises from the fact that the a posteriori distribution of random fields on spins classified according to the ramp on which they turn up is significantly modified from the uniform distribution given in Equation (II.1). Indeed, one of our immediate object is to calculate this distribution.

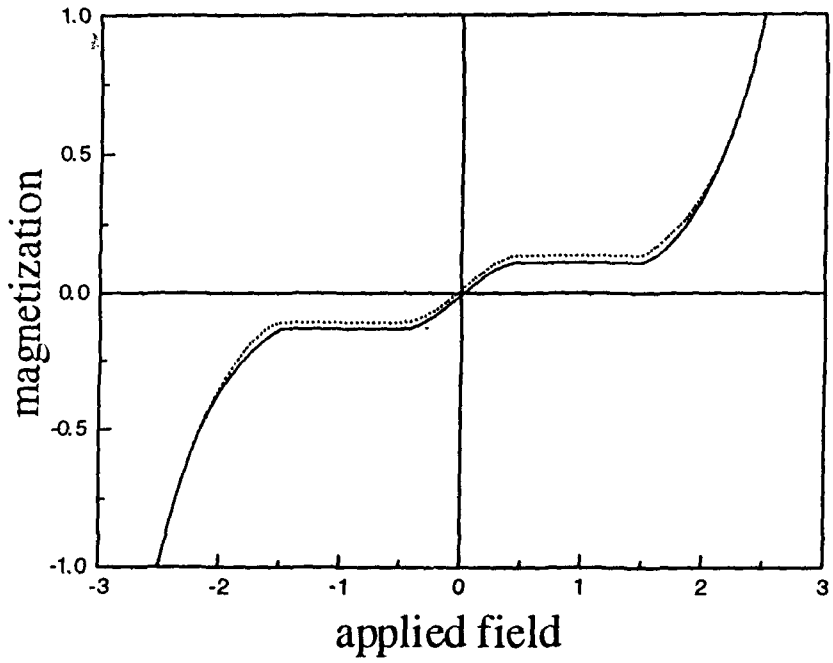

Fig.II.1: Magnetization $m(h_a)$ in an applied field h_a for an anti-ferromagnetic RFIM $J=-1$, obtained from a simulation of 10^3 spins averaged over 10^3 realizations of the random field distribution of which $2\Delta = 1$. The solid line shows the magnetization in an increasing field . The broken line shows the return half of the hysteresis loop. The data in increasing field is separated into five parts along the applied field: Ramp-I ($h_a = -2|J| - \Delta$ to $h_a = -2|J| + \Delta$); Plateau-I ($h_a = -2|J| + \Delta$ to $h_a = -\Delta$) ; Ramp-II ($h_a = -\Delta$ to $h_a = +\Delta$); Plateau-II ($h_a = +\Delta$ to $h_a = 2|J| - \Delta$) ; and Ramp-III ($h_a = 2|J| - \Delta$ to $h_a = 2|J| + \Delta$). Theoretical expressions obtained in this thesis have been superposed on the simulation curve and the two are indistinguishable.

CHAPTER– III

III. Ramp – I

III.1 Introduction

Magnetization on ramp-I was determined earlier [57] by exploiting a similarity between this problem and the problem of random sequential adsorption (RSA) [62]. The rate equations of the RSA problem were used to determine $m(h_a)$ on ramp-I, but they could not determine $m(h_a)$ on ramp-II and ramp-III. Here , we rederive the result for ramp-I by a different approach which can be extended to ramp-II as well.

We start with a large negative applied field $(h_a = -\infty)$ when all spins are down and increase the applied field slowly. At the start of ramp-I, i.e. at $h_a = -2|J| - \Delta$, the spin with the largest positive quenched field becomes unstable and flips up. As the applied field continues to increase, the spin with the next largest quenched field turns up unless it happens to be next to a spin which is already up. In this case the spin which turns up next is the one with the largest quenched field from among the spins with both neighbors down.

Consider an arbitrary point on ramp-I at an applied field $h_a = -2|J| - h$. In the following, the field h will be used more frequently than h_a. In general, the field h will be given by the relation

$h = -h_a \; mod \; 2|J|$, so that on each ramp it has the same range as the random field $-\Delta \le h \le \Delta$.

At an applied field $h_a = -2|J| - h$ all spins with quenched random field $h_i > h$ are relaxed, and a fraction of them are up. The fraction of sites with $h_i > h$ is given by

$$p(h) = \int_h^{\Delta} p(h_i) dh_i = \frac{\Delta - h}{2\Delta} \qquad \text{(III.1)}$$

The fraction of spins which are up on ramp-I at $h_a = -2|J| - h$ is given by

$$P_{\uparrow}^{I} = \frac{1}{2}\left[1 - e^{-2p}\right] \qquad \text{(III.2)}$$

III.2 Screening Pairs

Let $P_{\downarrow\downarrow}^{I}$ be the probability (per site) of finding a pair of adjacent down spins on ramp-I at the applied field $h_a = -2|J| - h$. On the lower half of the hysteresis loop, a pair of adjacent sites that have remain unflipped shield the evolution of the chain on one side of the pair from that on the other side. We therefore call it a pair of screening sites. The probability $P_{\downarrow\downarrow}^{I}$ can be calculated as follows. Imagine coloring all sites with $h_i > h$ black, and all sites with $h_i < h$ white. Consider two adjacent down spins A and B shown in Figure (III.1). The

sites A and B can be both white, both black , or mixed. Given that A is down, it is clear that the state of B can only be influenced by the evolution of the system to the right of B. Similarly, given that B is down, the state of A can only be influenced by the evolution of the system to the left of A. We shall refer to this as the principle of conditional independence [63][1]. It requires

$$P^{I}_{\downarrow\downarrow} = P(A \downarrow | B \downarrow) P(B \downarrow | A \downarrow) \qquad \text{(III.3)}$$

where $P(A \downarrow | B \downarrow)$ is the probability that spin at site A is down given that spin at B is down, and $P(B \downarrow | A \downarrow)$ is the probability that B is down given that A is down. We take up the calculation of $P(B \downarrow | A \downarrow)$. If B is a white site, $P(B \downarrow | A \downarrow) = 1$ because the white sites have not been relaxed from their initial state. If B is a black site and the site to the right of B is a white site then $P(B \downarrow | A \downarrow) = 0$. In general $P(B \downarrow | A \downarrow)$ depends on the length of the string of black sites to the right of B. Suppose B is a black site, and there are (n-1) additional black sites to the right of B. In this case, the probability P^{n}_{B} that B is down satisfies the following recursion relation,

$$P^{n}_{B} = \frac{1}{n} P^{n-2}_{B} + \left(1 - \frac{1}{n}\right) P^{n-1}_{B} \qquad \text{(III.4)}$$

[1] Also see Ref. [62] for a detailed discussion of the screening property of this class of problems.

The rationale for the above recursion relation is as follows. Let the black site farthest from B on the right be labeled as the n-th site. Any of the n sites could flip first. The probability that the n-th site flips first is

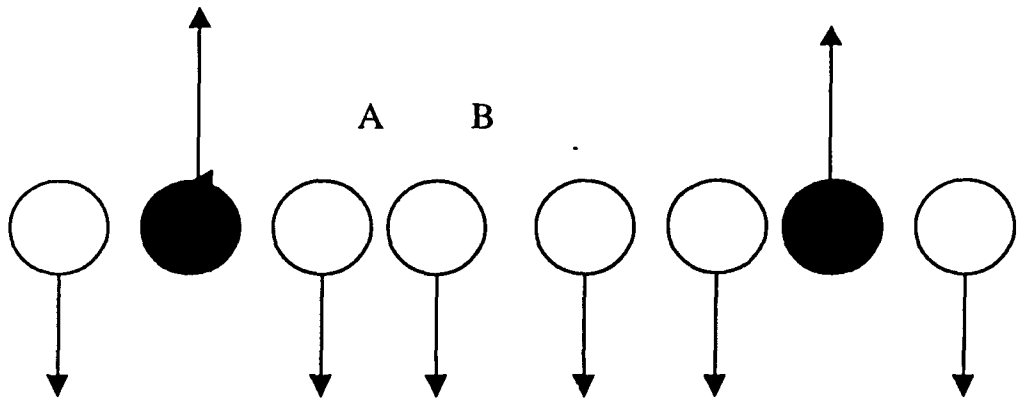

Fig.III.1: Spins on ramp-I in an applied field $-2|J|-h$. Filled circles show sites with $h_i > h$. The probability per site of a doublet (two adjacent down spins) such as AB is equal to e^{-2p}, where p is the fraction of filled circles on the infinite lattice.

therefore equal to $\frac{1}{n}$. If this happens, *(n-1)* th site is prevented from flipping up on ramp-I. The probability that B is down is now reduced to the probability that the end point of a chain of *(n-2)* black sites is down i.e. P_B^{n-2} . This accounts for the first term in equation (III.4). The probability that n-th site is not the first site to flip up is equal to $\left(1-\frac{1}{n}\right)$. Given this situation, the probability that B is down is equal to the

probability that the end of a string of *(n-1)* black sites is down. This accounts for the second term in equation (III.4). We can rewrite the recursion relation (III.4) as

$$\left(P_B^n - P_B^{n-1}\right) = -\frac{1}{n}\left[P_B^{n-1} - P_B^{n-2}\right] \tag{III.5}$$

It has the solution,

$$P_B^n = \sum_{m=0}^{n} \frac{(-1)^m}{m!} \tag{III.6}$$

Summing over various possible values of n with appropriate weight, we get

$$P_B = \sum_{n=0}^{\infty}\sum_{m=0}^{n} \frac{(-1)^n}{m!} p^n (1-p)$$

$$= \sum_{m=0}^{\infty} \frac{(-1)^m}{m!}(1-p)\sum_{n=m}^{\infty} p^n$$

$$= \sum_{m=0}^{\infty} \frac{(-p)^m}{m!} = e^{-p} \tag{III.7}$$

Thus,

$$P_{\downarrow\downarrow}^{I} = e^{-2p} \tag{III.8}$$

III.3 Magnetization on Ramp-I

Let $P_{\downarrow}^{I}$ be the probability per site of finding a down spin and $P_{\downarrow\uparrow}^{I}$ the probability per site of finding a down spin which is followed by an up spin. Clearly,

$$P_{\downarrow}^{I} = P_{\downarrow\downarrow}^{I} + P_{\downarrow\uparrow}^{I} = 1 - P_{\uparrow}^{I} \tag{III.9}$$

Keeping in mind that on ramp-I an up spin must be preceded (as well as followed) by a down spin, we get. $P_{\downarrow\uparrow}^{I} = P_{\uparrow}^{I}$. Thus,

$$P_{\uparrow}^{I} = 1 - P_{\downarrow\downarrow}^{I} - P_{\uparrow}^{I}$$

or,

$$P_{\uparrow}^{I} = \frac{1}{2}\left[1 - P_{\downarrow\downarrow}^{I}\right] = \frac{1}{2}\left[1 - e^{-2p}\right] \tag{III.10}$$

The magnetization on ramp-I is given by

$$m^{I}(h) = 2P_{\uparrow}^{I}(h) - 1 = -e^{-2p(h)} \tag{III.11}$$

Equation (III.11) has been superposed on the simulation data for ramp-I shown in Figure (II.1). The fit between the simulation and theory is so good that the two curves are indistinguishable from each other on the scale of Figure (II.1). The exact value of the magnetization on plateau-I is equal to $-\frac{1}{e^2}$ which is approximately equal to -0.135.

CHAPTER– IV

IV. Ramp-II

IV.1 Plateau-I

Plateau-I forms the initial state for the development of ramp-II. It contains down spins in singlets and doublets punctuated by up spins. The down spins were relaxed on ramp-I but did not turn up because the then applied field was not strong enough to turn up spins with at least one neighbour up. The singlets have two neighbours up, and the applied field on ramp-II is still not strong enough to turn them up. They have to wait for their turn on ramp-III. On the other hand, each spin in a doublet has one neighbour up and one down. It therefore experiences zero net field from its neighbours. The net field on a doublet spin is simply the sum of the random field h_i on its site and the applied field $h_a = -h$. It turns up when $h_a + h_i \geq 0$, or $h_i \geq h$. Note that the random field is bound in the range $-\Delta < h_i < +\Delta$. Therefore an applied field smaller than $-\Delta$ is sufficiently negative to pin down all doublets. This is the reason for the plateau in the magnetization for applied fields in the range $(-2|J| + \Delta) < h < -\Delta$. In each doublet, the spin with the larger quenched field h_i flips up on ramp-II when the applied field reaches a value such that $h_i \geq h$. The spin with the smaller quenched field then

becomes a singlet which does not flip up before ramp-III. Thus, in order to find the form of ramp-II, we need to find the a posteriori distribution of quenched random fields on the doublets.

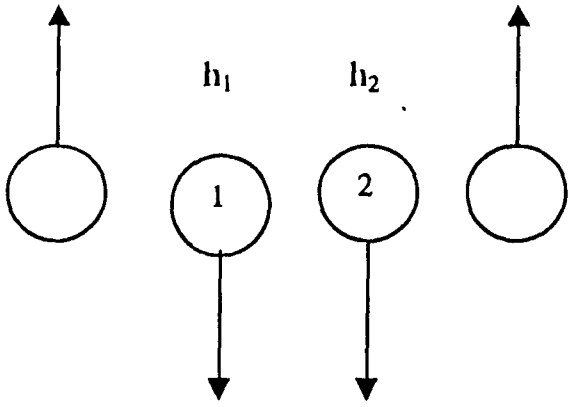

Fig.IV.1: A doublet on plateau-I: h_1 and h_2 are the quenched fields on the doublet sites 1 and 2.

Consider a doublet on plateau-I as shown in Figure (IV.1).The doublet sites are denoted as 1 and 2, and the quenched random fields on these sites are h_1 and h_2. The probability (per site) of finding a doublet on plateau-I is easily obtained from equation (III.8) by putting $p=1$. It is equal to $\frac{1}{e^2}$. We now calculate the probability distribution for h_1 and h_2. The distribution of h_1 and h_2 will be identical if the evolution of the system on the two sides of the doublet is similar to each other. We assume this to be the case for now, although we shall examine a more

general situation later. In order to obtain the desired probability distribution, consider the system on ramp-I when all spins are relaxed upto an arbitrary applied field $-2|J|-h$. At this point, the probability per site for finding a doublet is $P^{I}_{\downarrow\downarrow} = e^{-2p}$, where p is fraction of sites with $h_i > h$ (black sites) on an infinite lattice.

$$p(h) = \frac{\Delta - h}{2\Delta}$$

It is often easier to think in terms of the fraction p. We therefore introduce similar fractions for the quenched fields given by the following relations.

$$p(h_i) = \frac{\Delta - h_i}{2\Delta}; (i = 1,2,.....)$$

Given that site 1 is down on ramp-I, the conditional probability that the adjacent site 2 is also down is equal to e^{-p} . Site 2 may be black ($h_2 > h$ or equivalently $p_2 < p$) with an a priori probability p, or white with an a priori probability $(1-p)$. If site 2 is white ($h_2 < h$), it must be down because white sites are yet to be relaxed. Thus, the conditional probability that the spin at site 2 is down, and the quenched field at site 2 is larger than h is given by

$$Prob(2\downarrow | 1\downarrow, p_2 < p) = [e^{-p} - (1-p)] \qquad \text{(IV.1)}$$

The probability that the quenched field h_2 lies in the range h and h-dh, or equivalently p_2 is in the range p and $p+dp$ can be obtained by taking the derivative of the above expression. We obtain,

$$Prob\ [p < p_2 < p + dp]dp = [1 - e^{-p}]dp \qquad \text{(IV.2)}$$

Similarly,

$$Prob\ [p < p_1 < p + dp]dp = [1 - e^{-p}]dp \qquad \text{(IV.3)}$$

We now address an issue which is crucial for determining ramp-II correctly. This concerns two adjacent doublets on plateau-I as shown in Figure (IV.2). Let h_1, h_2, h_3, h_4 and h_5 denote the quenched fields at sites 1, 2, 3, 4, and 5 respectively. If $h_2 > h_1$, and $h_4 > h_5$, then spins at sites 2, 3, and 4 will be up at some value of the applied field on ramp-II. When this happens, i.e. when a triplet of up spins is created on ramp-II, the central spin at site 3 becomes unstable and it flips down. It stays down till the system reaches ramp-III. In order to take this effect into account, we must know the probability per site of observing two adjacent doublets on plateau-I, and also the distribution of fields at sites 2 and 4.

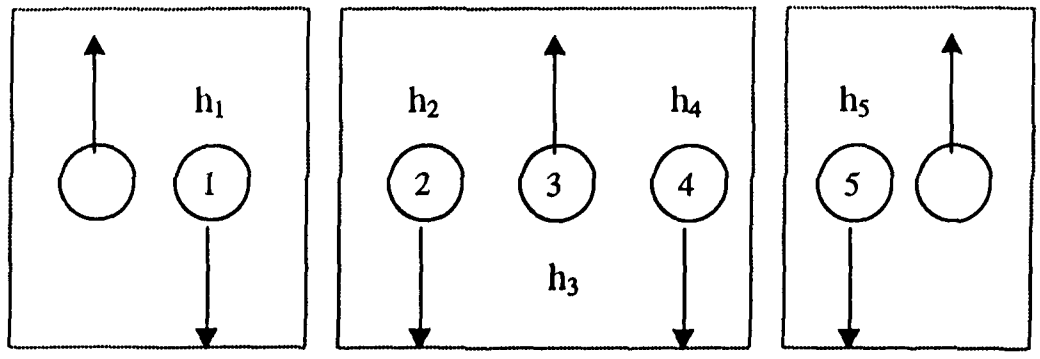

Fig.IV.2: Two adjacent doublets on Plateau-I: Each doublet separates the lattice into two parts whose evolution histories on Ramp-I are independent of each other. Evolutions inside each dash box is shielded from outside. The probability that spin at site 3 flips up on Ramp-I is therefore equal to $\frac{1}{3}$. Given this, the probability that the spins at site 1 and 5 remain down all along Ramp-I is equal to $\frac{1}{e}$ each. The shielding property of the boxes can also be used to determine a posteriori distribution of random fields h_1, h_2, h_3, h_4, *and* h_5.

A doublet on plateau-I has an important property. It separates the lattice into two parts (one on each side of the doublet) which have evolved uninfluenced by each other on ramp-I. Thus, we can separate Figure (IV.2) into three parts as enclosed in the dashed boxes. Evolution inside each box has remained shielded from the outside on ramp-I. The evolution in the middle box requires that site 3 flips up before site 2 or site 4. The probability for this event is equal to $\frac{1}{3}$. Given this event, the probability that spins at sites 1 and 5 remain down all along ramp-I

is each equal to $\frac{1}{e}$ .Thus the probability per site of observing two adjacent doublets on plateau-I is equal to $\frac{1}{3e^2}$. Note that it is quite different from the square of the probability of finding a single doublet!

The shielding property of the dashed boxes in Figure (IV.2) can also be used to calculate the a posteriori distribution of fields h_1, h_2,...,h_5. The distribution of h_1 and h_5 is the same as obtained above for a doublet with similar evolution on the two sides (Figure IV.1).

$$Prob(p \le p_1 \le p+dp)dp = [1-e^{-p}]dp \qquad \text{(IV.4)}$$

and ,

$$Prob(p \le p_5 \le p+dp)dp = [1-e^{-p}]dp \qquad \text{(IV.5)}$$

We now turn to the distributions of h_2, and h_4. Suppose, in the middle box in Figure (IV.2), the central spin at site 3 is up when all sites in the system with quenched fields $h_i \ge h$ (black sites) have been relaxed. This necessarily means that $h_3 \ge h$, i.e. site 3 is a black site, but sites 2 and 4 have other options. Site 3 will be up with probability $\frac{1}{3}p^3$ if 2 and 4 are both black, probability $p\,(1-p)^2$ if 2 and 4 are both white, and $(1-p)\,p^2$ if 2 and 4 are mixed. Thus the probability of

observing two adjacent doublets with the up spin separating them having field $h_3 \geq h(p_3 \leq p)$ is given by

$$P_{\downarrow\downarrow\uparrow\downarrow\downarrow}(p_3 \leq p) = \left[\frac{1}{3}p^3 + p(1-p)^2 + (1-p)p^2\right]\frac{1}{e^2} \qquad \text{(IV.6)}$$

In order to calculate the distribution of h_2 and h_4, it is convenient to write the distributions of the smaller and the larger of these two fields separately. Without any loss of generality, we can assume

$$h_2 = min\,(h_2\ ,\ h_4) \text{ and } h_4 = max(h_2\ ,\ h_4)$$

If $h_2 \geq h$, then we have $h_3 \geq h_4 \geq h$ as well. Thus the fraction of adjacent doublets on plateau-I with h_2, h_3, and h_4 all greater than an arbitrary h is given by

$$P_{\downarrow\downarrow\uparrow\downarrow\downarrow}(p_3 \leq p_4 \leq p_2 \leq p) = \frac{p^3}{3}\frac{1}{e^2} \qquad \text{(IV.7)}$$

The above equation gives the cumulative fraction of $p_2 \leq p$ sites. The fraction of sites in the range $p + dp \geq p_2 \geq p$ can be obtained by differentiating the above expression. We get,

$$P_{\downarrow\downarrow\uparrow\downarrow\downarrow}(p \leq p_2 \leq p + dp) = p^2\frac{1}{e^2} \qquad \text{(IV.8)}$$

The distribution of h_4 is obtained similarly. We find,

$$P_{\downarrow\downarrow\uparrow\downarrow\downarrow}(p \leq p_4 \leq p + dp) = 2p(1-p)\frac{1}{e^2} \qquad \text{(IV.9)}$$

Given that we have a pair of adjacent doublets, the probability densities of the quantities p_1, p_2, p_4, and p_5 (each normalized to unity) are given by:

$$\rho_1(p_1) = e[1 - e^{-p_1}] \tag{IV.10}$$

$$\rho_2(p_2) = 3p_2^2. \tag{IV.11}$$

$$\rho_4(p_4) = 6p_4(1 - p_4) \tag{IV.12}$$

$$\rho_5(p_5) = e[1 - e^{-p_5}] \tag{IV.13}$$

In the following, we focus on adjacent doublets which create up triplets on ramp-II. These are the objects with $h_2 \geq h_1$ and $h_4 \geq h_5$. At this stage, we can determine the lower and the upper bound on these objects at any point on ramp-II when spins with $h_i \geq h$ have been relaxed. Suppose we order the adjacent doublets in the order of increasing h_2 or increasing h_4. Note that a sequence in increasing h_2 does not posses any particular order in h_4, and vice versa. The lower bound is given by the fraction of objects with $h \geq h_2 \geq h_1$ (h_4 being free to have any value in the range $h_2 \leq h_4 \leq \Delta$).We obtain

$$\int_0^p \rho_2(p_2)dp_2 \int_{p_2}^1 \rho_1(p_1)dp_1$$

$$= (6 + 6p + 3p^2)e^{1-p} + (1 + e)p^3 - \frac{3}{4}ep^4 - 6e$$

$$= \left[16 - \frac{23}{4} e \right] \quad (\text{at } p = 1) \quad = 0.369 \ (\textit{approximately}) \qquad \text{(IV.14)}$$

Thus a minimum of approximately 37 % adjacent doublets will give rise to (unstable) up triplets on ramp-II.

Similarly, the fraction of adjacent doublets with $h \geq h_4 \geq h_5 \geq -\Delta$ is given by

$$\int_0^p p_4(p_4)\,dp_4 \int_{p_4}^1 p_5(p_5)\,dp_5$$

$$= (1+e)p^2(3-2p) - 2ep^3 + \frac{3}{2}ep^4 + 6e - 6(1+p+p^2)e^{1-p}$$

$$= \left[\frac{13}{2} e - 17 \right] \quad (\text{at } p = 1) \quad = 0.668 \ (\textit{approximately}) \qquad \text{(IV.15)}$$

This gives the upper bound. No more than approximately 67 % of the adjacent doublets can create (unstable) up triplets on ramp-II.

IV.2 Magnetization on Ramp-II

Ramp-II is determined by the combination of two opposite terms. The dominant term is the increase in magnetization due to the decrease in the number of doublets. When a doublet disappears, it adds an extra up spin in the system which increases the magnetization. Occasionally, a disappearing doublet creates a string of three up spins. A triplet of up spins is unstable on ramp-II, and the central spin of the triplet flips

down as soon as the triplet is created. This decreases the magnetization. In the following, we calculate the above two terms separately.

Refer to Figure (IV.1) for calculating the first term. The probability that the doublet shown in the Figure (IV.1) disappears when spins with $h_i \geq h$ are relaxed is given by

$$P_{\uparrow\uparrow}^{II} = \frac{2}{e^2} \int_0^p \rho(p_1) dp_1 \int_{p_1}^1 \rho(p_2) dp_2$$

The factor $\frac{1}{e^2}$ is the probability per site of finding a doublet shown in Figure (IV.1). The factor 2 takes care of the fact that either h_1 or h_2 may flip up first. The integrals are written on the assumption that the spin at site 1 flips up first. Together they give the probability that $h_1 \geq h$, and $h_2 \leq h_1$. Note that when a doublet disappears, a pair of adjacent up spins is created. This is the reason for the choice of the subscript on $P_{\uparrow\uparrow}^{II}$. The superscript indicates that the probability refers to ramp-II. We obtain,

$$P_{\uparrow\uparrow}^{II} = \frac{1}{e^2} - \left[\left(1 + e^{-1}\right) - \left(p + e^{-p}\right)\right]^2 \qquad \text{(IV.16)}$$

We now calculate the fraction of (unstable) up triplets formed in the system when all spins with $h_i \geq h$ have been relaxed on ramp-II. Let us

refer to Figure (IV.2). Recall that $h_2 \le h_4$ in this figure. We want the probability that $h_2 \ge h_1, h_4 \ge h_5$, and $h_2 \ge h$. This is given by,

$$P^{II}_{\uparrow\uparrow\uparrow} = \frac{1}{3e^2}\int_0^p \rho(p_2)dp_2 \int_{p_2}^1 \rho(p_1)dp_1 \left[\frac{\int_0^{p_2} \tilde{\rho}(p_4)dp_4 \int_{p_4}^1 \rho(p_5)dp_5}{\int_0^{p_2} \tilde{\rho}(p_4)dp_4} \right] \quad \text{(IV.17)}$$

The first factor is the probability per site of finding the object shown in Figure (IV.2). The next two integrals give the probability that $h_2 \ge h$, and $h_1 \le h_2$. The quantity in the square brackets is understood as follows: When h_2 is in the range h and $h+dh$, h_4 can be anywhere in the range h_2 to Δ. Let $\tilde{\rho}(h_4)$ be the density of h_4 in this range. Clearly,

$$\rho_2(h_2) = \int_{h_2}^{\Delta} \tilde{\rho}_4(h_4)\frac{dh_4}{2\Delta} \quad \text{(IV.18)}$$

or,

$$\rho_2(p_2) = \int_0^{p_2} \tilde{\rho}_4(p_4)dp_4 \quad \text{(IV.19)}$$

Thus,

$$\tilde{\rho}_4(p_4) = \frac{d\rho_2(p_2)}{dp_2} \quad \text{(IV.20)}$$

or,

$$\tilde{\rho}_4(p_4) = 6p_4 \qquad \text{(IV.21)}$$

We get,

$$P^{II}_{\uparrow\uparrow\uparrow} = \frac{1}{3}\left[\frac{3}{2} + \frac{6}{e} - 6\left(1+\frac{1}{e}\right)p + 3p^2 + \left(1+\frac{1}{e}\right)^2 p^3 - \frac{5}{4}\left(1+\frac{1}{e}\right)p^4 + \frac{2}{5}p^5 - \left\{6\left(1+\frac{1}{e}\right) - 6p - 3\left(1+\frac{1}{e}\right)p^2 + 2p^3\right\}e^{-p} + \left(\frac{9}{2}+3p\right)e^{-2p}\right]$$

We show in Figure (IV.3) a comparison of the above expression with a result from the simulation. As may be expected, the agreement between the simulation and the theory is excellent.

Incidentally, an interesting quantity is the ratio of (unstable) up triplets at the end of ramp-II to the fraction of adjacent doublets at the start of ramp-II. We noted in the previous section that this ratio must lie approximately in the range *0.369* to *0.668*. If there were no correlations between adjacent doublets, this ratio would be equal to $\frac{1}{4}$, because the events $h_2 > h_1$, or $h_4 > h_5$ would occur with probability $\frac{1}{2}$. The exact value of the probability that $h_4 \geq h_5 \geq -\Delta$ and $h_2 \geq h_1 \geq -\Delta$ is given by

$$P^{II}_{\uparrow\uparrow\uparrow} = \frac{1}{3e^2}\left[\frac{11}{2} + \frac{7}{4}e - \frac{27}{20}e^2\right] \qquad \text{(IV.22)}$$

The quantity in the square bracket is approximately equal to 0.281. We have checked this result rather carefully numerically, and it is born out by the simulations. Finally, putting the various terms together, the probability of an up spin on ramp-II is given by

$$P^{II}_{\uparrow}(p) = P^{I}_{\uparrow}(1) + P^{II}_{\uparrow\uparrow}(p) - P^{II}_{\uparrow\uparrow\uparrow}(p) \qquad \text{(IV.23)}$$

The magnetization on ramp-II is given by

$$m^{II}(p) = 2P^{II}_{\uparrow}(p) - 1 \qquad \text{(IV.24)}$$

This expression has been superposed on the numerical data for ramp-II shown in Figure (II.1). The agreement between the numerical data and the theory is extremely good. The exact value of the magnetization on plateau-II, and its numerical estimate are given by

$$m^{II}(1) = \left[\frac{27}{30} - \frac{7}{6}e^{-1} - \frac{8}{3}e^{-2}\right] = 0.109 \ (approximately) \qquad \text{(IV.25)}$$

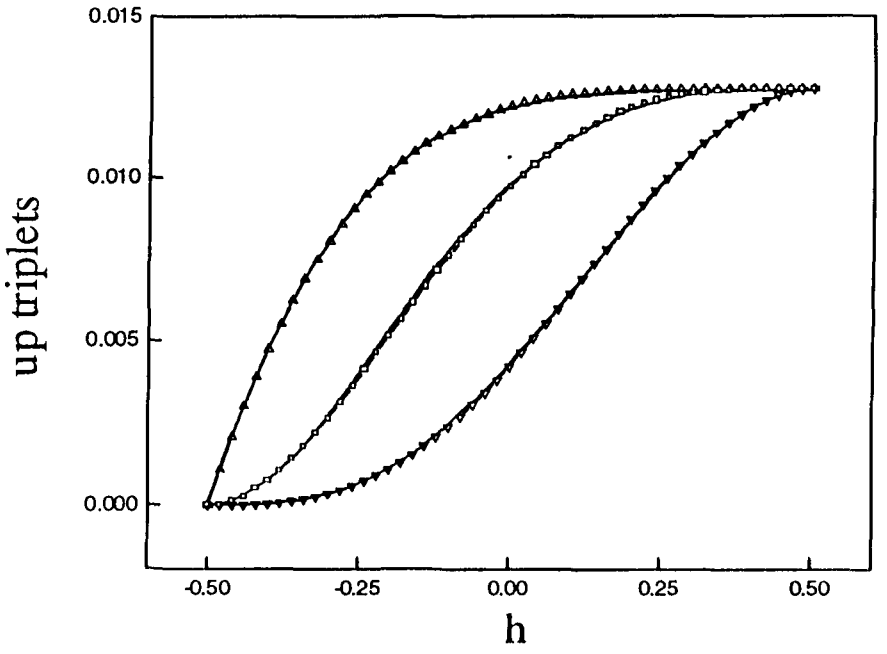

Fig.IV.3: Unstable up triplets on Ramp-II with $h_2 \geq h$ (lower curve) ; $h_4 \geq h$ (middle curve) ; and $h_3 \geq h$ (upper curve). Refer to Figure (IV.2) for h_2, h_4, *and* h_3. The simulation data is shown by lines, and the symbols on each line show the corresponding theoretical prediction.

CHAPTER– V

V. Ramp-III

V.1 Plateau-II

Each down spin on plateau-II is a singlet. However, there are three different classes of singlets: the singlets formed on ramp-I; singlets formed on ramp-II by a vanishing doublet; and finally the singlets formed on ramp-II by the unstable central spin of an up triplet flipping down. Each class is characterized by its own a posteriori distribution of the random field.

Let us denote the three distribution densities by ρ_1^{II}, ρ_2^{II}, and ρ_3^{II} respectively. Let P_1^{II}, P_2^{II}, and P_3^{II} denote the cumulative populations in each class when spins with $h_i \geq h$ have been relaxed on ramp-III. We have,

$$P_i^{II}(p) = \int_0^p \rho_i^{II}(p_i) dp_i, \; i = 1, 2, 3. \qquad \text{(V.1)}$$

It is useful to think of the singlets in each class as being black $(h_i \geq h)$, or white $(h_i \leq h)$, where h_i is the quenched random field at the singlet site, and h is an arbitrary reference field. In order to calculate ramp-III, we need only the populations of black singlets in

each class given by $P_i^{II}(p)$. If needed, one can obtain the density $\rho_i^{II}(p)$ by differentiating $P_i^{II}(p)$ with respect to p.

The fraction of black singlets created on ramp-I is given by,

$$P_1^{II}(p) = p - \frac{1}{2}\left[1 - e^{-2p}\right] - \frac{2}{e}\left[e^{-p} - (1-p)\right] \qquad \text{(V.2)}$$

The explanation of the above equation is as follows. Imagine ordering the sites of the lattice in order of decreasing quenched field on the site. When all sites with $h_i \geq h$ have been relaxed, the fraction of the relaxed sites is equal to p (the black sites). This fraction is made of the up sites (the second term on the right), black doublet sites (the last term), and the black singlets. Hence the equation for $P_1^{II}(p)$. The last term is written as follows. In each doublet, there are two sites from which we can choose one. This accounts for the factor 2. The quantity in the square bracket gives the probability that the chosen site is black, and $\frac{1}{e}$ is the probability that the other site can have any allowed value of the quenched field.

The fraction of black singlets generated by vanishing doublets on ramp-II is given by,

$$P_2^{II}(p) = \left[e^{-p} - (1-p)\right]^2 \qquad \text{(V.3)}$$

The above equation is easily understood. It is the probability that both sites of the doublet are black. If both sites of the doublet are black, the one with higher random field must flip up on ramp-II, leaving us with a singlet on plateau-II which is black.

The fraction of black singlets created by unstable triplets requires the calculation of triplets. We have calculated the fraction of triplets as they are formed on ramp-II. What we need now is a similar but different calculation. The point can be understood with a reference to Figure (IV.2). Recall that $h_3 \geq h_4 \geq h_2$. On ramp-II, we needed the fraction of triplets with $h_2 \geq h$, because the formation of triplets is controlled by this threshold. The restoration of the triplets on ramp-III is controlled by the condition $h_3 \geq h$. In the earlier calculation, sites 2, 3, and 4 were all black sites. In the calculation needed now, only site 3 is black. Sites 2, and 4 are white, and we want $h_1 \leq h_2$, and $h_5 \leq h_4$. The probability for this event is given by

$$P_3^{II}(p) = 2\int_0^p dp_3 \int_{p_3}^1 dp_4 \int_{p_4}^1 \left[1 - e^{-p_5}\right] dp_5 \int_{p_4}^1 dp_2 \int_{p_2}^1 \left[1 - e^{-p_1}\right] dp_1$$

As a check, we note that

$$2\int_{p_3}^1 dp_4 \int_{p_4}^1 dp_2 = (1 - p_3)^2$$

Thus, the double integral gives the probability that sites 2 and 4 are white {compare with the second term on the right hand side of Equation (IV.6)}. The extra terms in $P_3^{II}(p)$ take into account the requirements $h_5 \le h_4$, and $h_1 \le h_2$.

$$P_3^{II}(p) = 2\int_0^p dp_3 \int_{p_3}^1 \left[1 + e^{-1} - p_4 - e^{-p_4}\right] dp_4 \int_{p_4}^1 \left[1 + e^{-1} - p_2 - e^{-p_2}\right] dp_2$$

We get,

$$P_3^{II}(p) = -\left(1 + \frac{2}{e}\right) + \left[\frac{1}{4} + \frac{2}{e} + \frac{4}{e^2}\right]p - \frac{1}{2}\left[1 + \frac{5}{e} + \frac{4}{e^2}\right]p^2 + \frac{1}{3}\left[\frac{3}{2} + \frac{4}{e} + \frac{1}{e^2}\right]p^3$$

$$-\frac{1}{4}\left[1 + \frac{1}{e}\right]p^4 + \frac{1}{20}p^5 + \left[1 + \frac{2}{e}\right]e^{-p} - \frac{2}{e}pe^{-p} + p^2e^{-p} + \frac{1}{2}\left[1 - e^{-2p}\right]$$

(V.4)

As a check we note that,

$$P_3^{II}(1) = \frac{1}{3e^2}\left[\frac{11}{2} + \frac{7}{4}e - \frac{27}{20}e^2\right]$$

This is the same as given by Equation (IV.22). As one may expect, the number of triplets with $h_3 \ge h$ is larger than triplets with $h_2 \ge h$, but the two merge at $h = -\Delta$ i.e. $p = 1$.

It is of some interest to calculate the number of triplets with $h_4 \geq h$ as well, although this quantity is not directly needed in the calculation of ramp-III. Denoting this quantity by $P_4^{II}(p)$, we get

$$P_4^{II}(p) = 2\int_0^p p_4 dp_4 \int_{p_4}^1 \left[1 - e^{-p_5}\right] dp_5 \int_{p_4}^1 dp_2 \int_{p_2}^1 \left[1 - e^{-p_1}\right] dp_1$$

Note that either h_2 or h_4 could have been the larger of the two fields although we have assumed that h_4 is the larger one. This accounts for the factor 2 on the right hand side. The factor p_4 comes from integrating p_3 over the range 0 to p_4. The other terms are self-explanatory.

We get[1],

$$P_4^{II}(p) = -\left[\frac{1}{2} + \frac{2}{e}\right] + \frac{1}{2}\left[1 + \frac{5}{e} + \frac{4}{e^2}\right]p^2 - \frac{2}{3}\left[\frac{3}{2} + \frac{4}{e} + \frac{1}{e^2}\right]p^3 + \frac{3}{4}\left[1 + \frac{1}{e}\right]p^4$$

$$-\frac{1}{5}p^5 + \left[\left(1 + \frac{2}{e}\right)(1 + p - p^2) + p^3\right]e^{-p} - \left[\frac{1}{2} + p\right]e^{-2p} \qquad \text{(V.5)}$$

It can be checked that $P_4^{II}(1)$ also reduces to the expression in Equation (IV.22) as may be expected. In Figure (IV.3), we have shown the theoretical expressions for $P_{\uparrow\uparrow\uparrow}^{II}(p)$, $P_3^{II}(p)$, and $P_4^{II}(p)$

[1] In the reference [59] in the expression (46), in the second-last term p^2 should be replaced by $-p^2$

along with the results from the simulations for the same quantities. The simulations were performed for a system of 10^3 spins, and averaged over 10^3 different realizations of the random field distribution. The agreement is excellent as may be expected from an exact analytic result. The agreement between the simulation and the theory also justifies (albeit post facto) the implicit assumption in our analysis that the system is self-averaging. The fact that simulations over a relatively small size of the system (10^3 spins) agree with the exact result is due to the super-exponential decay of correlations in this system [62].

V.2 Magnetization on Ramp –III

Plateau-II forms the ground state for the evolution of ramp-III in an increasing applied field. The ground state has solitary down spins dispersed in a sea of up spins. The net field on a singlet is equal to $-2|J|+h_i+h_a$. This lies in the range $[-2|J|-\Delta+h_a]$ to $[-2|J|+\Delta+h_a]$. Therefore, the singlets begin to turn up at $h_a=2|J|-\Delta$, and are all up at $h_a=2|J|+\Delta$. These limits mark the beginning and the end of ramp-III. The shape of ramp-III is determined by the fraction of up spins at applied fields between these limits. We take an arbitrary value of the applied field $h_a=-2|J|-h$

on ramp-III, and calculate the fraction of singlets which are up at this field. In other words, we calculate the fraction of singlets with $h_i \geq h$ or equivalently $p_i \leq p$, where

$$p_i = \frac{\Delta - h_i}{2\Delta}$$

As discussed, the singlets on plateau-I fall into three categories. In category (1) are the singlets which were created on ramp-I. The fraction of singlets which belong to this category, and whose quenched field is greater than h is given by,

$$P_1^{II}(p) = p - \frac{1}{2}\left[1 - e^{-2p}\right] - \frac{2}{e}\left[e^{-p} - (1-p)\right] \qquad \text{(V.6)}$$

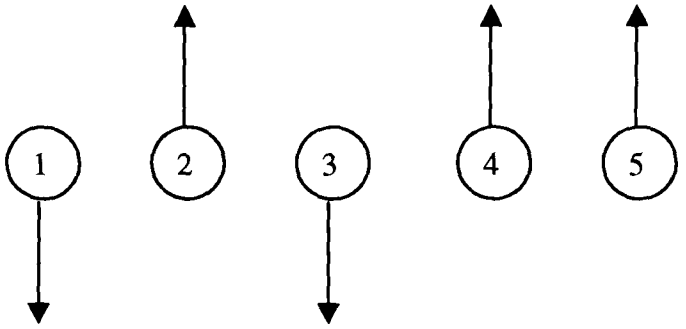

Fig.V.1: A singlet (site 3) with one next nearest neighbour down (site 1), and one next nearest neighbour up (site 5). When the singlet turns up at an applied field h_a the spin at site 2 stays up if $\Delta \leq |J|$, but the spin at site 3 will flip down when the spin at site 2 flips up on ramp-III. This process creates a new singlet on Ramp-III.

In category (2) are the singlets which were created on ramp-II by a vanishing doublet. The fraction of singlets in this category whose quenched field is greater than h is equal to,

$$P_2^{II}(p)=\left[e^{-p}-(1-p)\right]^2 \tag{V.7}$$

Finally, category (3) singlets are those that were created on ramp-II by the central spin of an unstable up triplet flipping down. The fraction of singlets in this category whose quenched field is larger than h is given by,

$$\begin{aligned} P_3^{II}(p)=&-\left(1+2e^{-1}\right)+\left[\frac{1}{4}+2e^{-1}+4e^{-2}\right]p \\ &-\frac{1}{2}\left[1+5e^{-1}+4e^{-2}\right]p^2+\frac{1}{3}\left[\frac{3}{2}+4e^{-1}+e^{-2}\right]p^3 \\ &-\frac{1}{4}\left[1+e^{-1}\right]p^4+\frac{1}{20}p^5+\left[1+2e^{-1}\right]e^{-p} \\ &-2pe^{-(1+p)}+p^2e^{-p}+\frac{1}{2}\left[1-e^{-2p}\right] \end{aligned} \tag{V.8}$$

The total fraction of singlets present on plateau-II whose quenched fields is larger than h is equal to,

$$P^{II}(p)=P_1^{II}(p)+P_2^{II}(p)+P_3^{II}(p) \tag{V.9}$$

The above equation gives the fraction of singlets which will turn up in an applied field $h_a=2|J|-h$ from among the singlets initially present on plateau-II. However, when these singlets turn up, some of

their nearest neighbours turn down. This process creates new singlets[2]. The newly created singlets turn up later at a higher applied field on ramp-III. We need to calculate the fraction of newly created singlets, and their restoration to the original state as function of the applied field before we can determine ramp-III.

V.3 Creation of New Singlets

In this section, we consider the circumstances in which the destruction of a singlet on ramp-III accompanies the creation of a new singlet. Consider a singlet in the ground state, say the spin at site 3 in Figure (V.1). Its nearest neighbours at sites 2 and 4 are up. A next nearest neighbour at site 1 is down, and the other next nearest neighbour at site 5 is up. Suppose the singlet just flips up on ramp-III at an applied field h_a, i.e. $h_3 - 2|J| + h_a = \varepsilon$, where $\varepsilon \geq 0$. The applied field at this point is $h_a = 2|J| - h_3 + \varepsilon$. We ask the question, could a nearest neighbour of the singlet flip down when the singlet flips up?

---

[2] Although the new singlets make the analysis of ramp-III somewhat tedious, but they save our model from an unphysical feature. If we neglect the new singlets, the two halves of the hysteresis loop cross each other twice so as to make a series of three subloops. In this case, one could engineer a violation of the second law of thermodynamics by running an engine over two of the subloops. However, the new singlets on ramp-III push down the lower half of the hysteresis loop and prevent the upper half from crossing it.

First, consider the nearest neighbour at site 2 in Figure (V.1). After site 3 has flipped up, site 2 has one nearest neighbour up and one down. Thus site 2 may flip down if $h_2 + h_a \leq 0$, or $h_2 \leq h_3 - 2|J| - \varepsilon$. However, this is not possible because h_2 and h_3 lie in the range $[-\Delta$ to $\Delta]$, and we are considering the case $\Delta \leq |J|$. Thus a nearest neighbour of a singlet which has both its nearest neighbours down will stay up when the singlet turns up as long as $\Delta \leq |J|$.

Next, consider the spin at site 4. After the singlet has turned up, site 4 has both its nearest neighbours up. It will turn down if $-2|J| + h_4 + h_a \leq 0$, or $h_4 \leq h_3 - \varepsilon$. If $h_4 \leq h_3$, site 4 will turn down when site 3 turns up. After site 4 has turned down, site 3 has one neighbour up and one down. The net field at site 3 is then $h_3 + h_a = 2|J| + \varepsilon$, which is positive. Thus site 3 will stay up after site 4 has turned down. We conclude that, when a singlet turns up, its nearest neighbour may turn down if that nearest neighbour has less quenched field than the singlet, and also if it had one nearest neighbour already up before the singlet turned up. Note that when site 4 turns down, it increases the upward field at site 5. There is no possibility of site 5 turning down as a result of site 4 turning down.

Consequently, a spin turning up on ramp-III does not cause any change in the state of spins beyond the nearest neighbours (absence of avalanches).

Before proceeding further, we rewrite the two rules which will guide us in the following analysis.

Rule-1: When a singlet turns up on ramp-III, its nearest neighbour stays up if the adjacent next nearest neighbour is down, and $\Delta \leq |J|$.

Rule-2: When a singlet turns up on ramp-III, its nearest neighbour turns down if both of the following conditions are satisfied:

(a) the adjacent next nearest neighbour is up, and

(b) the nearest neighbour has less quenched field than the singlet.

The next question is, in what circumstances, the quenched field on a nearest neighbour of a singlet on plateau-II can be smaller than the quenched field on the singlet. We examine various possible cases. Suppose the singlet in question was created on ramp-II by the destruction of a doublet. For example, look at Figure (V.1) again and suppose sites 2 and 5 were up, and 3 and 4 were down on plateau-I. This requires $h_3 \leq h_2$ and $h_4 \leq h_5$. Let $h_3 \leq h_4$ without any loss of generality. In this case, site 4 will turn up on ramp-II. When site 3 turns up on ramp-III, no new singlet can be created because both

nearest neighbours of site 3 have a larger quenched field than site 3 (Rule-2).

Next, let us assume that the singlet in question was created on ramp-II by the unstable central spin of an up triplet flipping down. The central spin of an up triplet flips up for the first time on ramp-I. It separates two adjacent doublets on plateau-I. Therefore, the quenched field on the central spin is larger than the quenched field on each of its nearest neighbours. The nearest neighbours of the central spin flip up on ramp-II (the central spin flips down at this event). Therefore each nearest neighbour of the central spin has a larger quenched field than the next nearest neighbour of the central spin which is adjacent to it. Consequently the central spin has a larger quenched field than each of its next nearest neighbours. When the central spin flips up for the second time on ramp-III, its next nearest neighbours are still down. Therefore there is no chance (Rule-2) for the nearest neighbours of the central spin to flip down when the central spin flips up on ramp-III.

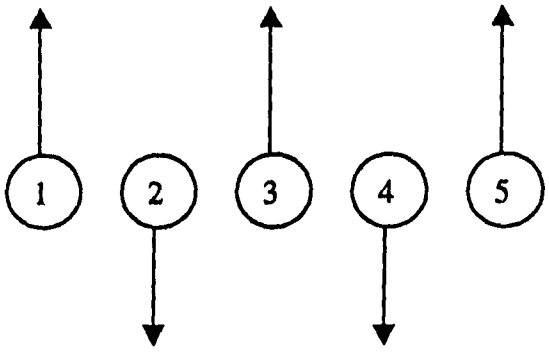

Fig.V.2: Two adjacent singlets on Plateau-I: If $h_2 = min\ (h_2\ ,\ h_4)$, and $h_3 \leq h_2$, then the spin at site 3 will flip down when the spin at site 2 flips up on Ramp-III. This process creates a new singlet on Ramp-III.

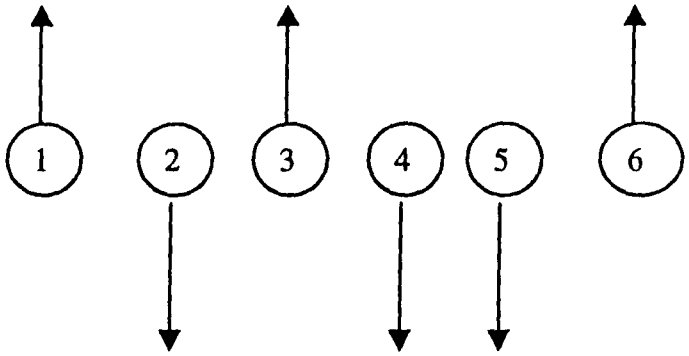

Fig.V.3: A singlet followed by a doublet on Plateau-I : If $h_4 \geq h_5$, and $h_3 \leq h_2$, then a new singlet will be created at site 3 when the spin at site 2 turns up on Ramp-III.

Having ruled that the destruction of a singlet created on ramp-II does not give rise to a new singlet on ramp-III, we are left with singlets created on ramp-I and present on plateau-I. When one of these singlets disappears on ramp-III, it may create a new singlet if

one of its nearest neighbours has a smaller quenched field than the singlet, and if the next nearest neighbour is up. We note that only one of the two nearest neighbours of a singlet on plateau-I can have a quenched field which is smaller than the singlet. A site which has a larger quenched field than both of its nearest neighbours must be up on plateau-I. Now consider a singlet on plateau-I as shown at site 2 in Figure (V.2). Let its nearest neighbour on the right (at site 3) have a smaller quenched field ($h_3 \leq h_2$). Site 4 must be down because there are no strings of up spins of length greater than unity on plateau-I. Site 5 may be up or down. The two possibilities for site 5 are depicted in Figures (V.2) and (V.3) respectively. In Figure (V.2), a singlet is followed by a singlet on plateau-I. In Figure (V.3), a singlet is followed by a doublet.

Consider Figure (V.2) first. What is the probability per site that such an object occurs on plateau-I? A singlet on plateau-I must be followed by a singlet or a doublet. It was shown that the probability per site of the occurrence of a doublet is equal to e^{-2}, and the probability that a doublet is followed by a doublet is equal to $\frac{1}{3}e^{-2}$. Therefore, the probability that a doublet is followed by a singlet (or

vice-versa) is equal to $\frac{2}{3}e^{-2}$. It was also shown that the probability of the occurrence of a singlet is equal to $\frac{1}{2}\left[1-3e^{-2}\right]$. Therefore, the probability per site that a singlet is followed by a singlet on plateau-I is equal to $\frac{1}{2}\left[1-\frac{13}{3}e^{-2}\right]$.

We have obtained above the probability of the occurrence of objects shown in Figure (V.2). Our immediate interest lies in a subset of these objects with $h_3 \leq min\,(h_2, h_4)$. This subset determines the creation of new singlets. Suppose $h_2 \leq h_4$. Then on ramp-III, site 4 will flip up before site 2. When site 2 flips up, site 3 will flip down because the conditions for the creation of a new singlet are fulfilled (Rule-2). In order to calculate the fraction of newly created singlets, we need to know the distribution of fields h_2, h_3, and h_4 . These may be obtained if one notes that sites 1 and 5 must have flipped up on ramp-I before site 3. Site 1 must have flipped up before site 3 because $h_1 \geq h_2 \geq h_3$ .Similarly, site 5 must have flipped up before site 3 because $h_5 \geq h_4$, $h_4 \geq h_2$, $h_2 \geq h_3$, and therefore $h_5 \geq h_3$.

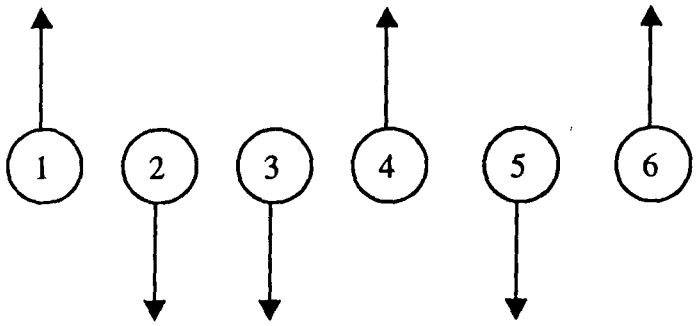

Fig.V.4: A doublet followed by a singlet on Plateau-I: If $h_3 \geq h_2$, and $h_4 \leq h_5$, then a new singlet will be created at site 4 when the spin at site 5 turns up on Ramp-III.

This proves that just before site 3 flipped up on ramp-I, sites 2, 3, and 4 formed a string of three down spins bordered by up spins at sites 1 and 5. The screening property discussed can be applied here to conclude that the distributions of h_2, and h_4 are independent of each other, and each is given by

$$Prob[p \leq p_2 \leq p+dp] = \left[1-e^{-p}\right]dp$$

$$Prob[p \leq p_4 \leq p+dp] = \left[1-e^{-p}\right]dp$$

where

$$p_i = \frac{\Delta - h_i}{2\Delta}$$

Given that h_2 lies in the range $[h \text{ to } h+dh]$, h_3 must be uniformly distributed in the range $[-\Delta \text{ to } h]$. Thus,

$$Prob[p \le p_3 \le p+dp] = dp \quad (\text{if } p_3 \ge p_2)$$

The contribution of Figure (V.2) to the fraction of newly created singlets when all sites with $h_i \ge h$ have been relaxed on ramp-III is given by[3],

$$P_4^{III}(p) = 2\int_0^p [1-e^{-p_2}]dp_2 \int_{p_2}^1 dp_3 \int_0^{p_2} [1-e^{-p_4}]dp_4$$

$$= \frac{3}{2} - 2p(1-p) - \frac{2}{3}p^3 - 2\left(1-p+p^2\right)e^{-p} + \frac{1}{2}(1-2p)e^{-2p} \qquad \text{(V.10)}$$

Consider Figure (V.3) next. It shows a singlet at site 2 followed by a doublet at sites 4 and 5. An identical contribution will come from a situation where the doublet occurs at sites 2 and 3, and the singlet at site 5 as shown in Figure (V.4). We work out the contribution from Figure (V.4) explicitly and then multiply it by a factor 2 to take into account the contribution from Figure (V.4). When site 2 flips up, site 3 will flip down if $h_3 \le h_2$, and if site 4 is up as well. Note that site 4 would have flipped up earlier on ramp-II if $h_4 \ge h_5$. If $h_5 \ge h_4$, site 5 would have flipped up on ramp-II.

[3] In Reference [60], Equation (9), the upper limit of the third integral is shown as p due to a typographical error. It should be p_2.

In this case there is no possibility of site 3 flipping down when site 2 flips up. The reason is as follows. The presence of a doublet at sites 4 and 5 on plateau-I means that $h_4 \leq h_3$ and $h_5 \leq h_6$. We must have $h_3 \leq h_2$ for the creation of a new singlet (Rule-2). If $h_4 \leq h_3$, and $h_3 \leq h_2$, then we have $h_4 \leq h_2$. Thus, when site 2 turns up on ramp-III, site 4 will be down, and one of the two conditions for the creation of a new singlet is not satisfied.

A similar reasoning as applied in the analysis of Figure (V.2) reveals that site 3 must have flipped up after sites 1 and 6. The distribution of fields at sites 2 and 5 in Figure (V.3) must be similar to the distribution of fields at sites 2 and 4 in Figure (V.2). The distribution of fields at sites 3 and 4 must be uniform over the interval $[-\Delta$ to $min(h_1, h_6)]$. Thus the contributions of Figures (V.3) and (V.4) to the fraction of newly created singlets when sites with $h_i \geq h$ have been relaxed on ramp-III is given by,

$$P_5^{III}(p) = 2\int_0^p \left[1-e^{-p_2}\right] dp_2 \int_{p_2}^1 dp_3 \int_{p_3}^1 dp_4 \int_{p_4}^1 \left[1-e^{-p_5}\right] dp_5$$

$$=\left(\frac{1}{3}+3e^{-1}\right)+\left(\frac{1}{3}+5e^{-1}\right)p-\left(\frac{1}{2}+2e^{-1}\right)p^2+\frac{1}{3}\left(1+e^{-1}\right)p^3-\frac{1}{12}p^4$$

$$+\left\{\left(\frac{4}{3}+3e^{-1}\right)-\left(1+2e^{-1}\right)p+e^{-1}p^2-\frac{1}{3}p^3\right\}e^{-p}-e^{-2p} \qquad \text{(V.11)}$$

V.4 Destruction of New Singlets

The destruction of newly created singlets on ramp-III can be analysed in a similar manner as their creation. For example, refer to Figure (V.2) again, and recall that $h_2 = min\ (h_2, h_4)$, and $h_3 \le h_2$. In this figure, the creation of new singlets when all sites with $h_i \ge h$ have been relaxed is determined by $h_2 \ge h$. The destruction of new singlets when all sites with $h_i \ge h$ have been relaxed is given by $h_3 \ge h$. The result is an integral similar to the expression for the creation of singlets. Only the limits of the integration are altered. We obtain[4],

$$P_6^{III}(p)=2\int_0^p dp_3\int_0^{p_3}\left[1-e^{-p_2}\right]dp_2\int_0^{p_2}\left[1-e^{-p_4}\right]dp_4$$

$$=\frac{1}{2}\left[1-e^{-2p}\right]-2pe^{-p}+p(1-p)+\frac{1}{3}p^3 \qquad \text{(V.12)}$$

Similarly, the contribution from Figures 3 and 4 is given by,

[4] In Reference [60], Equation (11), the upper limit of the third integral is shown as p_3 due to a typographical error. It should be p_2.

$$P_7^{III}(p)=2\int_0^p dp_3\int_0^{p_3}\left[1-e^{-p_2}\right]dp_2\int_{p_3}^1 dp_4\int_{p_4}^1\left[1-e^{-p_5}\right]dp_5 \qquad \text{(V.13)}$$

$$=2e^{-1}-\left(1+4e^{-1}\right)p+\left(\frac{3}{2}+3e^{-1}\right)p^2-\left(1+\frac{2}{3}e^{-1}\right)p^3+\frac{1}{4}p^4$$

$$-\left\{\left(1+2e^{-1}\right)-2\left(1+e^{-1}\right)p+p^2\right\}e^{-p}+e^{-2p} \qquad \text{(V.14)}$$

Putting the various terms together, the probability that a randomly chosen spin on the chain is up on ramp-III is given by

$$P_{\uparrow}^{III}(p)=P_{\uparrow}^{II}(1)+P_1^{III}(p)+P_2^{III}(p)+P_3^{III}(p)$$

$$-P_4^{III}(p)-P_5^{III}(p)+P_6^{III}(p)+P_7^{III}(p) \qquad \text{(V.15)}$$

The magnetization on ramp-III is given by,

$$m^{III}(h)=2P_{\uparrow}^{III}(p)-1 \qquad \text{(V.16)}$$

After some simplification, we obtain

$$m^{III}(h)=-\left\{\frac{13}{30}-\frac{53}{6}e^{-1}+\frac{8}{3}e^{-2}\right\}+\left\{\frac{11}{6}-18e^{-1}+8e^{-2}\right\}p$$

$$-\left(1-5e^{-1}+4e^{-2}\right)p^2+\frac{1}{3}\left(1+2e^{-1}+2e^{-2}\right)p^3$$

$$-\left\{\left(\frac{8}{3}+10e^{-1}\right)-\left(2+4e^{-1}\right)p-\left(4-2e^{-1}\right)p^2-\frac{2}{3}p^3\right\}e^{-p}+(4+2p)e^{-2p}$$

(V.17)

The above expression has been superposed on the simulation data in Figure (II.1). The agreement is excellent. The analytic result is indistinguishable from the simulation on the scale of Figure (II.1).

V.5 Hysteresis Loop

So far, we have analyzed the magnetization $m(h_a)$ in increasing applied field. We have shown that the analytic result agrees with the simulation rather well. The magnetization $m_R(h_a)$ in decreasing field (return loop) is related to $m(h_a)$ by a symmetry of the model, i.e. $m_R(h_a) = -m(-h_a)$. Thus we have implicitly determined the return loop as well. The return loop has been shown in Figure (II.1) by a broken line. The hysteresis in the anti-ferromagnetic RFIM is rather small, and the two halves of the hysteresis loop lie very close to each other. In order to show them more clearly, we have plotted in Figure (V.5) the separation between the two halves of the hysteresis loop versus the applied field. To be precise, we have plotted $[m(h_a) - \overline{m}]$ and $[m_R(h_a) - \overline{m}]$ vs. h_a, where $\overline{m} = \frac{1}{2}[m_R(h_a) + m(h_a)]$.

As we may expect, the agreement between the theoretical expression and the simulation is excellent on the scale of Figure (V.5) as well. In Figure (V.5) the simulation data was obtained from a system of 10^3 spins, and averaged over 10^3 independent realizations

of the random field distribution. The set of applied fields where the spins flip on each half of the hysteresis loop is of course different for each realization of the random field distribution. Therefore, the average over different realizations requires a judgement on how to group the data. We divided the entire range of the applied field from $[-2|J|-\Delta$ to $2|J|+\Delta]$ into 3×10^3 sections (bins) of equal width. The data in each bin was averaged separately. The simulation data shown in Figure (V.5) is a much sparser set of data (in order not to crowd the figure). We have shown the simulation data at intervals of $\delta h_a = 0.1$, and the theoretical expression at intervals of $\delta h_a = 0.01$ (joined by a continuous line on the lower half and a broken line on the upper half of the hysteresis loop).

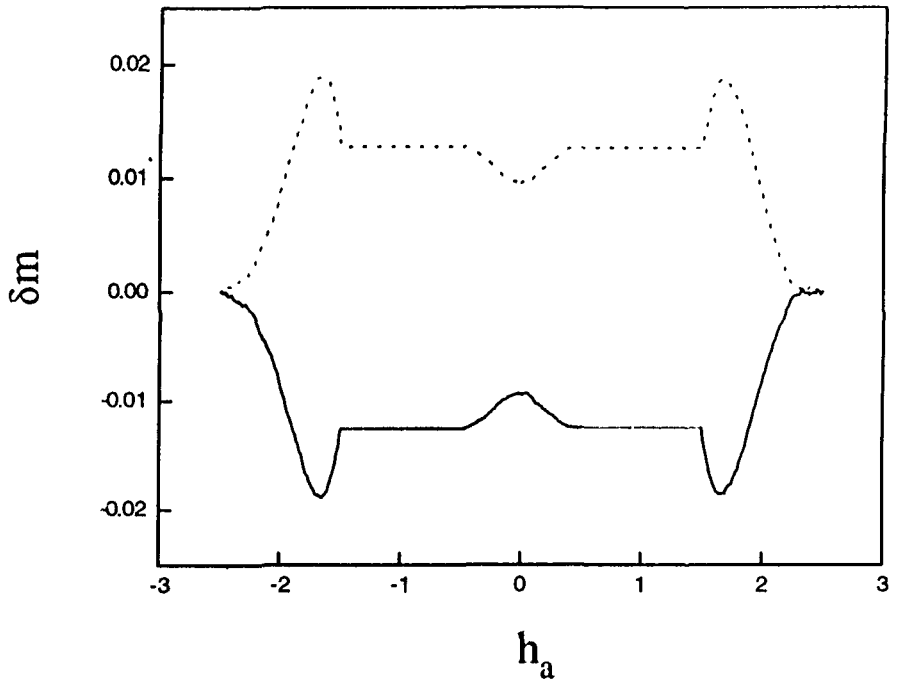

Fig.V.5: Separation between the two halves of the hysteresis loop in figure (II.1) has been magnified by plotting it relative to the average value of the two halves. The solid line shows $\delta m = [m - \overline{m}]$, and the broken line $\delta m = [m_R - \overline{m}]$ vs. the applied field h_a ; $\overline{m} = \frac{1}{2}[m_R + m]$; m and m_R are the magnetizations at applied field h_a in increasing and decreasing field respectively.

V.6 Discussion

We have considered the zero-temperature dynamics of a one-dimensional anti-ferromagnetic random field Ising model, and obtained an analytic solution of the model if the following conditions apply:

1) All spins are down initially, and the applied field is swept from $h_a = -\infty$ to $h_a = +\infty$ infinitely slowly. The solution is also applicable by symmetry to the case when all spins are up in the initial state, and h_a is decreased from $h_a = +\infty$ to $h_a = -\infty$.

2) The random field has a uniform bounded distribution in the interval $[-\Delta \text{ to } +\Delta]$. So far we have considered the case $\Delta \leq |J|$. The simplifying feature of this case is that the increasing applied field exhausts all strings of down spins of length three or more (ramp-I) before working on strings of down spins of length two (ramp-II). Similarly, strings of down spins of length one (singlets) are turned up (ramp-III) only after the doublets are finished.

The second condition mentioned above has been adopted essentially for simplicity. It serves to illustrate the method of solution with a minimum of algebraic detail.

The restriction to an initial state where spins are either all down or all up appears to be necessary so far. A similar difficulty is encountered in the ferromagnetic random field Ising model [52]. The relaxation dynamics of the ferromagnetic model is qualitatively different from that of the anti-ferromagnetic model. The relaxation process in the ferromagnetic model is abelian, while in the anti-

ferromagnetic model it is not. We have made some progress in the methods of analytic solutions in both cases, but a qualitatively new idea appears to be needed in extending these methods to an arbitrary initial state.

CHAPTER–VI

VI. Large Disorder

VI.1 Introduction

The preceding chapters have presented the solution of the zero-temperature hysteresis in the AFRFIM in the case that the half-width of the rectangular distribution of the random field is less than the magnitude of the exchange interaction, i.e. $\Delta \leq |J|$. In this case, on the lower half of the hysteresis loop, a site with two nearest neighbours up flips up only after all sites with one nearest neighbour up have flipped up. Similarly, a site with one nearest neighbour up flips up after all sites with no nearest neighbours up have been exhausted. Thus the problem of calculating the lower hysteresis loop breaks up into three separate problems of calculating ramp-I, ramp-II, and ramp-III. This simplification is not available in the case of large disorder, i.e. if $\Delta \geq |J|$.

We have spent considerable time and thought attempting to generalize the results for $\Delta \leq |J|$ to the case of large disorder, i.e. $\Delta \geq |J|$. However, the progress in this direction has been less than satisfactory. We understand some of the new features of the relaxation dynamics that arise when $\Delta \geq |J|$ and we have attempted to incorporate these into our analysis. However, as discussed below, there remains a

slight discrepancy between our theoretical expressions and the corresponding simulations. This makes us suspect that there may be additional effects which have not been included in our analysis so far, or our treatment of the effects that are included is not entirely accurate. We are constrained by various factors to leave this issue for further research, and we present here the results which we have obtained so far.

VI.2 Screening Pairs

In Chapter – IV we discussed the importance of a pair of adjacent sites which screen the evolution of the spin chain on one side of the pair from the evolution on the other side. In other words, the screening pair of adjacent sites divides the chain into two halves that have evolved uninfluenced from each other. In general there is a finite fraction of screening pairs on the chain. The screening pairs punctuate the entire chain into a number of segments that have evolved independently of each other. On the lower half of the hysteresis loop, starting with a state with all spins down, the screening pairs of sites at an applied field h are simply pairs of adjacent sites which have not flipped up till the application of field h. In Chapter (III) we calculated the fraction of such pairs when $\Delta \leq |J|$. We now take up the same calculation in the case of large disorder i.e. $\Delta \geq |J|$.

Consider Figure (VI.1) shown below.

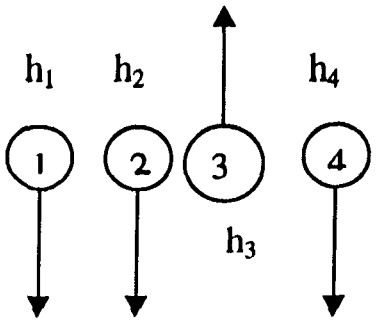

Fig VI.1

Given that site 1 is down at an applied field h, we want the probability that the adjacent site 2 is down as well. Let this conditional probability be denoted by $p_{\downarrow\downarrow}(h)$. Given that site 1 is down, the event that site 2 is down can occur in the following two ways. Either site 3 is down or site 3 is up. If site 3 is up, there are again two cases: either site 3 flipped up under a p_0– process i.e. site 3 flipped up when sites 2 and 4 were both down, or site 3 has flipped under a p_1 – process i.e. site 3 flipped up when site 4 was up and site 2 was down. Notice that the flipping up of site 3 under a p_1 – process while site 2 is down is not allowed if $\Delta \leq |J|$.

Let us write

$$p_{\downarrow\downarrow}(h) = p^{a}_{\downarrow\downarrow}(h) + p^{b}_{\downarrow\downarrow}(h) \qquad \text{(VI.1)}$$

where $p^{a}_{\downarrow\downarrow}(h)$ corresponds to the event that site 3 is either down or it has flipped up under a p_0 – process. Similarly, $p^{b}_{\downarrow\downarrow}(h)$ gives the contribution of the event in which site 3 flips up under a p_1 – process.

The term $p^{a}_{\downarrow\downarrow}(h)$ is similar to the case of small Δ with site 2 staying down on ramp – II. We get,

$$p^{a}_{\downarrow\downarrow}(h)=e^{-p_0(h)}-\left[e^{-p_1(h)}-\{1-p_1(h)\}\right] \qquad \text{(VI.2)}$$

The first term on the right-hand side gives the probability that site 2 remains down under a p_0 – process whether site 3 has flipped up or stays down under a p_0 – process. The second term in square bracket gives the probability that site 2 flips up under a p_1 – process after site 3 has flipped up. This term was calculated in Chapter – III, and we simply take this result from there.

Next, let us consider the event shown in Figure (VI.2).

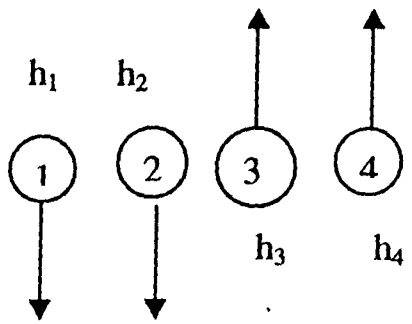

Fig.VI.2

Here we have,

$$h_4 + 2|J| + h > 0 \qquad \text{(VI.3)}$$

$$h_3 + 2|J| + h > 0 \qquad \text{(VI.4)}$$

$$h_2 + 2|J| + h > 0 \qquad \text{(VI.5)}$$

$$h_4 > h_3 > h_2 \qquad \text{(VI.6)}$$

$$h_3 + h > 0 \qquad \text{(VI.7)}$$

$$h_2 + h < 0 \qquad \text{(VI.8)}$$

Thus each of the sites, site 1, site 2, site 3, or site 4 can flip up at an applied field h with both nearest neighbours down, but site 4 flips first, then site 3. Site 2 remains down because it does not have sufficient random field on it to flip up if one of its nearest neighbours is up.

Given that site 1 is down, the conditional probability that site 2 is down in this event is given by

$$p^{b}_{\downarrow\downarrow}(h) = \int_{-2|J|-h}^{-h} \frac{dh_2}{2\Delta}\left[e^{-p_2(-h_2)} - \{1 - p_2(-h_2)\}\right] \qquad \text{(VI.9)}$$

The limits on the integral over the random field h_2 follow from Equations (VI.5) and (VI.8). The maximum applied field that can be applied without causing site 2 to turn up is equal to $h = -h_2$. The quantity in the square bracket in Equation (VI.9) gives the probability that the field h_3 is large enough to satisfy Equations (VI.3), (VI.4) and

(VI.7). Note that after site 4 has flipped up under a p_0 – process, the a posteriori distribution of the field h_3 is determined as discussed earlier in Chapter (III). Another point to be noted is that the lower limit in the integral in Equation (VI.9) is to be set equal to $-\Delta$ if $-2|J|-h<-\Delta$. Thus we get

$$p^{b}_{\downarrow\downarrow}(h)=e^{-p_2(h)}-e^{-\tilde{p}_1(h)}-[\tilde{p}_1(h)-p_2(h)]\left[1-\frac{1}{2}\{\tilde{p}_1(h)+p_2(h)\}\right] \tag{VI.10}$$

where

$$\tilde{p}_1(h)=p_1(h) \quad \text{if} \quad -2|J|-h\geq-\Delta$$

$$=1-\frac{|J|}{\Delta} \quad \text{if} \quad -2|J|-h\leq-\Delta$$

Finally, for $\Delta\geq|J|$, the probability of finding a pair of adjacent sites which remain unflipped up to an applied field on the lower hysteresis loop is given by

$$P_{\downarrow\downarrow}(h)=\left[p^{a}_{\downarrow\downarrow}+p^{b}_{\downarrow\downarrow}\right]^2 \tag{VI.11}$$

In Figure (VI.3a) we show a comparison between the theoretical prediction given by Equation (VI.11), and simulation data obtained from a system of 10^3 spins (averaged over 10^4 independent realizations of the random field distribution) for $\Delta=3$. The agreement between the

theoretical result and the simulation looks reasonable but there is a slight discrepancy in Figure (VI.3a) which becomes visible in Figure (VI.3b). Figure (VI.3b) is a magnified version of Figure (VI.3a) in the range $-1 \le h \le 3$. Qualitatively similar (mostly smaller) discrepancies arise for other values of Δ larger than $|J|$. We have not been able to resolve these discrepancies so far. Our educated guess is that the simulation results are more reliable than the theoretical expressions. For the case of small disorder $\Delta \le |J|$, our simulations have matched perfectly with the theoretical expressions even on magnified scales (hence magnified figures have not been shown for $\Delta \le |J|$).

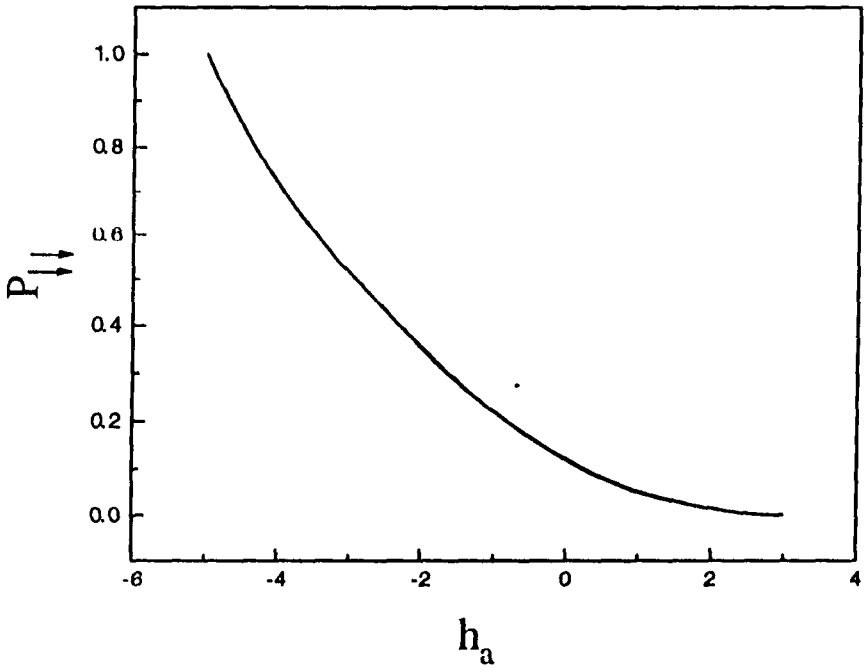

Fig. VI.3a: Fraction of screening pairs vs. applied field for $\Delta = 3|J|$. The theoretical expression is shown by a continuous line and the result of simulation (10^3 spins averaged over 10^4 distinct realization of the random field) are shown by dots. The simulation results are not distinguishable from the theoretical expressions on the scale of the above figure.

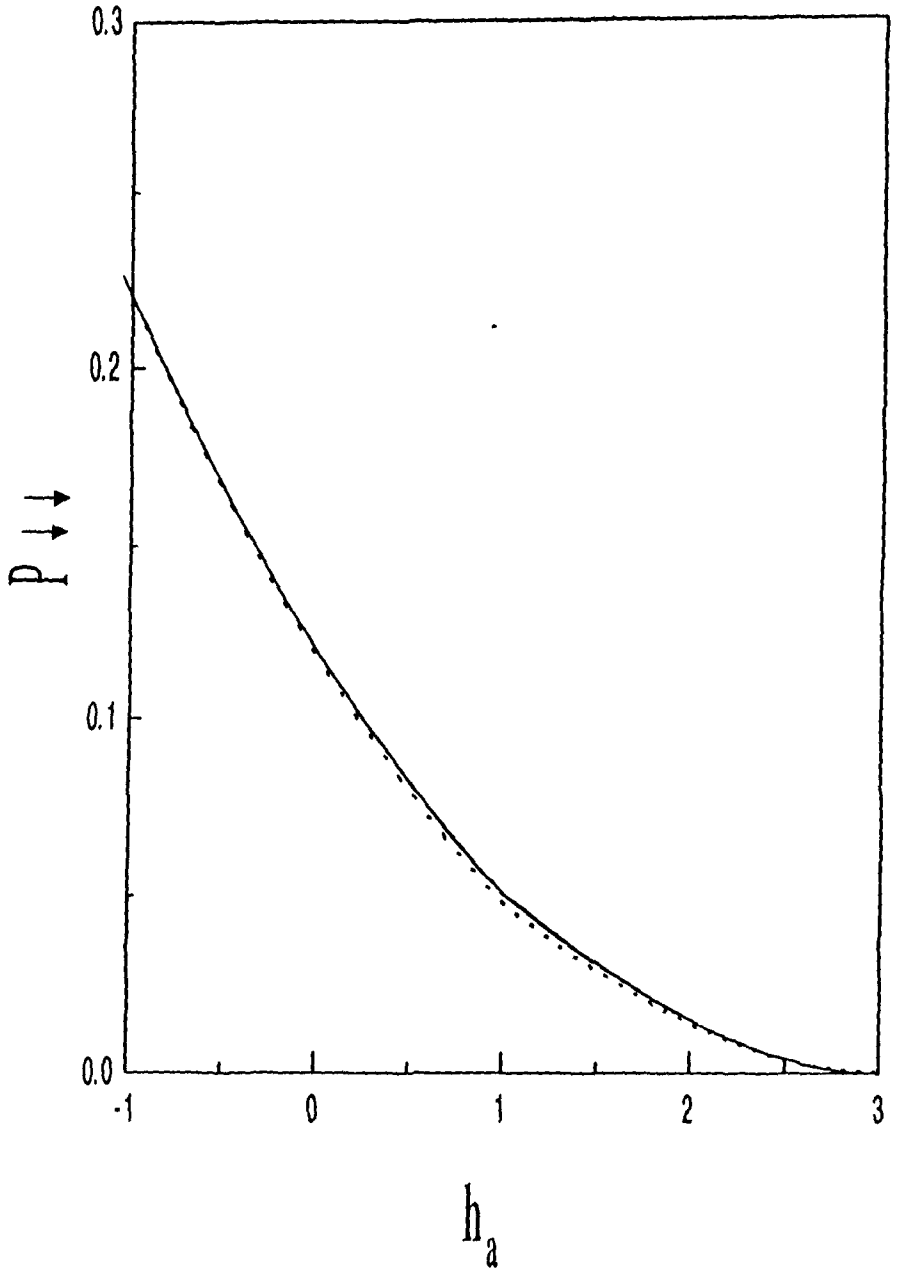

Fig. VI.3b: This is Figure (VI.3a) magnified in the range $-1 \leq h_a \leq 3$ to bring out the small discrepancy between the theoretical expression and the simulation result.

VI.3 Magnetization on Lower Hysteresis Loop

We now take up the calculation of the magnetization curve on lower half of the hysteresis loop. The basic quantity to be computed is $P_{\uparrow}(h)$- the fraction of sites that are up at an applied field h. The magnetization is given by

$$m_l(h)=2P_{\uparrow}(h)-1$$

The magnetization on the upper half of the loop may be obtained from $m_l(h)$ by a symmetry of the model as indicated in section V.5.

As is the case of $\Delta \leq |J|$, there are two main issues that need to be addressed. The a posteriori distribution of random fields at unflipped sites next to a flipped site needs to be determined. Secondly, a small fraction of sites which flip up in an increasing applied field, flip down when their nearest neighbours flip up. These sites make consecutively a positive, negative, and again a positive contribution to the magnetization on the lower hysteresis loop.

Consider the sites which flip three times on the lower hysteresis loop. In the case of $\Delta \leq |J|$, all sites which flip three times, flip up the first time on ramp-I. Some of these sites flip down on ramp-II, and others on ramp-III. Finally, all sites which flip three times flip up the second time on ramp-III. For $\Delta \geq |J|$, the magnetization curve no longer

breaks up into three distinct ramps. However, it is possible to retain the earlier formulation with a slight change of nomenclature. For $\Delta > |J|$, all sites which flip three times, flip for the first time under a p_0 – process; i.e. they flip up the first time when none of their nearest neighbours is up. A small set of these sites flip down under a p_1 – process. More precisely these sites flip down when their nearest neighbour flips up under a p_1 – process. The nearest neighbour in question has one nearest neighbour up and one nearest neighbour down when it flips up. In other words, a site flipping up under a p_1 – process causes its nearest neighbour to flip down. Earlier we had called this event the creation of a singlet from an unstable up triplet on ramp-II. The up triplet is created by a p_1 – process and is unstable against the central site flipping down. The remaining sites which flip three times flip down under a p_2 – process. Finally, all sites which flip three times flip up for the second time under a p_2 – process, i.e. they flip up for the second time when both of their nearest neighbours are up.

The form of a posteriori distribution of random field at an unflipped site next to a site that has flipped up under a p_0 – process is not affected if p_1 – processes commence before all p_0 – processes have been completed. Similarly, the distribution of fields at singlets formed

by both nearest neighbours flipping up under a p_0 – process has the same form for $\Delta \geq |J|$, as for $\Delta \leq |J|$. In Chapter (V), we stated two rules governing the sites which turn down under a p_2 – process.

Rule-1 stated that "when a singlet turns up on ramp-III, its nearest neighbour stays up if the adjacent next nearest neighbour is down, and $\Delta \leq |J|$." This rule is modified to the following form:

Rule-1 (modified): When a singlet turns up under a p_2 – process, its nearest neighbour stays up if the adjacent next nearest neighbour is down.

The omission of the inequality $\Delta \leq |J|$ in the modified rule needs an explanation. Consider Figure (V.2); when site 2 turns up at an applied field h, we have $-2|J| + h + h_2 = 0$. After site 2 has turned up the net field at site 3 is equal to $h_3 + h = h_3 + 2|J| - h_2$. The net field at site 3 is necessarily negative if $\Delta \leq |J|$. If $\Delta > |J|$, we may have $h_3 + 2|J| - h_2 < 0$, if $h_2 > h_3 + 2|J|$. But in this case, site 2 would have flipped up before site 3 considering that there is no longer a restriction that that all p_0 – processes must be completed before p_1 – processes can commence. Hence, we get the modified rule-1 as stated above. Similarly, the modified form of rule-2 becomes:

Rule-2 (modified): When a singlet turns up under a p_2 – process, its nearest neighbour turns down if both of the following conditions are satisfied:

(a) the adjacent next nearest neighbour is up, and

(b) the nearest neighbour has less quenched field than the singlet.

It can be proven on similar lines as in Chapter (V) that only the destruction of a singlet that was created entirely by a p_0 – process (ramp-I in the nomenclature of $\Delta \leq |J|$) can cause a neighbouring site to flip down. With these provisions, we write

$$P_{\uparrow} = P_{\uparrow}^{0} + P_{\uparrow}^{11} - P_{\uparrow}^{12}$$

$$+ P_{\uparrow}^{21} + P_{\uparrow}^{22} + P_{\uparrow}^{23}$$

$$- P_{\uparrow}^{24} - P_{\uparrow}^{25} + P_{\uparrow}^{26} + P_{\uparrow}^{27}$$

The various terms occurring in the above equation are described in the following. We give a key to each expression. The key is given in the form of a brief description of the term, a diagram, an integral for the contribution of the term. The integrals can be performed as done earlier in Chapter (V).

Following symbols have been used to in order to simplify the integral expressions:

$$f(y)=e^{-y}-(1-y)$$

$$g(y)=e^{-p_0}-[e^{-y}-(1-y)]$$

$$u(y)=1-e^{-y}$$

$$p_0 = p_0(h)$$

$$p_1 = p_1(h)$$

$$p_2 = p_2(h)$$

The variable of integration y (subscripts are used to denote the variable at a particular site as indicated in the diagram) is related to the random field at the site. It denotes the probability for the site to flip up under a p_0, p_1 or p_2 - process (as appropriate) at an applied field h.

$P_{\uparrow}^{0}(h)$: spins turning up under a p_0 – process.

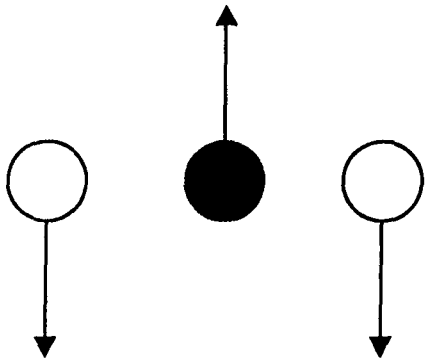

$$P_{\uparrow}^{0}(h)=\int_{0}^{p_0} e^{-y}dy\, e^{-\dot{y}}$$

$$= \frac{1}{2}\left[1 - e^{-2p_0}\right]$$

Explanation: The central spin turns up under a p_0-process with probability dy. The nearest neighbour on each site is down with probability e^{-y}.

$P_{\uparrow}^{11}(h)$: spins turning up under a p_1 – process.

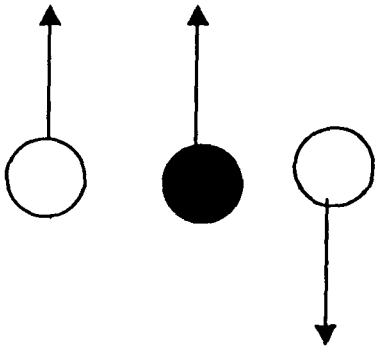

$$P_{\uparrow}^{11}(h) = \int_0^{p_1} u(y)\,dy\; g(y)$$

$$= 2e^{-p_0}\left[e^{-p_1} - (1 - p_1)\right] - \left[e^{-p_1} - (1 - p_1)\right]^2$$

Explanation: The central spin turns up under a p_1-process with probability dy. The nearest neighbour on the left has already flipped up with probability $u(y)$ and the neighbour to the right is down with probability $g(y)$.

$P_{\uparrow}^{12}(h)$: spins turning down under a p_1 – process (unstable up triplets).

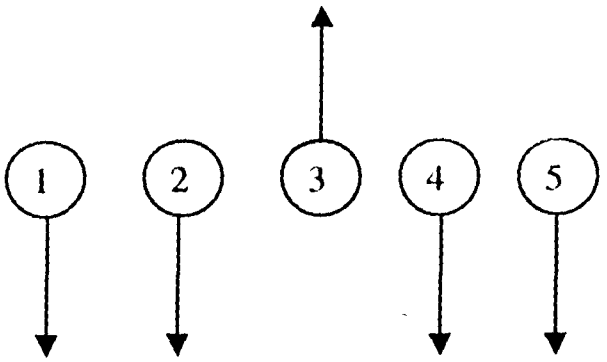

$$P_{\uparrow}^{12}(h) = 2\int_0^{p_1} g(y_2)\, dy_2 \int_0^{y_2} g(y_4)\, dy_4 \int_{y_{3min}}^{y_4} dy_3$$

where $y_{3min} = y_2 - \frac{|J|}{\Delta}$, $y_{3min} = 0$ if $y_2 < \frac{|J|}{\Delta}$.

Explanation: The term is written on the assumption that $h_2 < h_4$. The case $h_2 > h_4$ makes an equal contribution, hence the factor 2 in front. The unstable up triplet is created when site 2 turns up; $g(y_2)$ gives the probability that site 2 turns up before site 1. Similarly $g(y_4)$ is the probability that site 4 turns up before site 5.

$P_{\uparrow}^{21}(h)$: spins turning up by a p_2 – process; (destruction of singlets created by a p_0 – process).

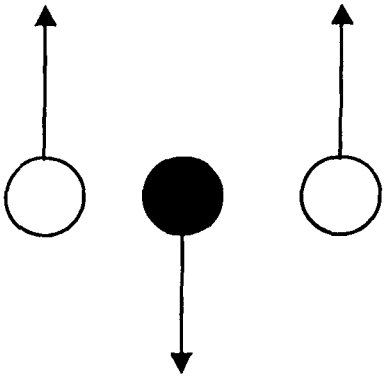

$$P_{\uparrow}^{21}(h) = \int_0^{p_2} u(y)\,dy\,[2u(p_0) - u(y)]$$

Explanation: The a posteriori field at the singlet is determined by the neighbour which flips up first. $u(y)$ is the probability for the first neighbour to flip up (before the applied field reached the value h), and $u(p_0)$ is the probability that the second neighbour also flips up by the time the applied field reaches the value h.

$P_{\uparrow}^{22}(h)$: spins turning up by a p_2 – process; (destruction of singlets created by a p_1 – process).

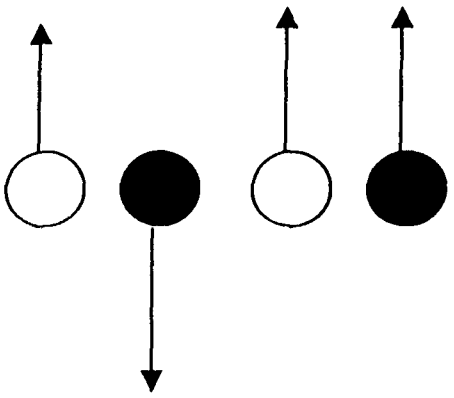

$$P_{\uparrow}^{22}(h) = 2\int_{0}^{p_2} u(y)\, dy\ f(y)$$

Explanation: $u(y)$ refers to the neighbour which flips up under a p_0 – process and $f(y)$ the neighbour which flips up under a p_1 – process.

$P_{\uparrow}^{23}(h)$: spins turning up by a p_2 – process; (destruction of singlets created by unstable up triplets).

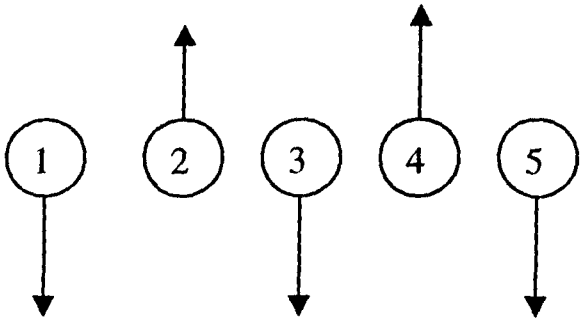

$$P_{\uparrow}^{23}(h) = 2\int_{0}^{p_2} dy_3 \int_{y_3}^{1} g(y_4)dy_4 \int_{y_4}^{y_{2max}} g(y_2)dy_2$$

where $y_{2max} = y_3 + \frac{|J|}{\Delta}$, $y_{2max} = 1$ if $y_3 + \frac{|J|}{\Delta} > 1$.

Explanation: The rationale for the above integral is similar to the integral expression for unstable triplets mentioned above.

$P_{\uparrow}^{24}(h)$: spins turning down by a p_2 – process.

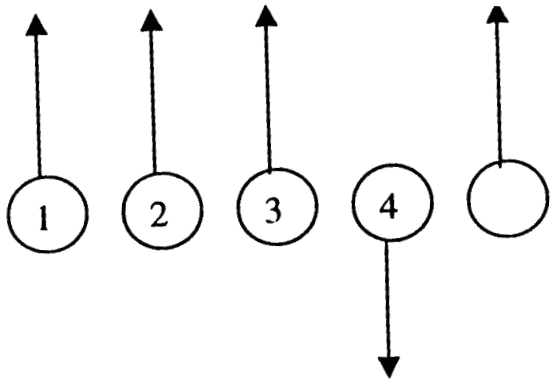

$$P_{\uparrow}^{24}(h) = 2\int_{0}^{p_2}(1-y)\cdot f(y)\,dy\;u(y)$$

Explanation: Similar to term $P_4^{III}(p)$ in Chapter (V).

$P_{\uparrow}^{25}(h)$: spins turning down by a p_2 – process.

$$P_{\uparrow}^{25}(h) = 2\int_{0}^{p_2} u(y_2)dy_2 \int_{y_2}^{1} dy_3 \int_{y_3}^{1} dy_4 \left[\frac{1}{e} - f(y_4)\right]$$

Explanation: Similar to term $P_5^{III}(p)$ in Chapter (V).

$P_{\uparrow}^{26}(h)$: spins turning up by a p_2 – process (destruction of singlets created by $P_{\uparrow}^{24}$).

$$P_{\uparrow}^{26}(h) = 2\int_{0}^{p_2} dy_3 \int_{0}^{y_3} u(y_2)\; f(y_2)\; dy_2$$

Explanation: Similar to term $P_6^{III}(p)$ in Chapter (V).

$P_{\uparrow}^{27}(h)$: spins turning up by a p_2 – process (destruction of singlets created by $P_{\uparrow}^{25}$).

$$P_{\uparrow}^{27}(h)=2\int_{0}^{p_2} dy_3\ f(y_3)\int_{y_3}^{1} dy_2\left[\frac{1}{e}-f(y_2)\right]$$

Explanation: Similar to term $P_7^{III}(p)$ in Chapter (V).

In Figure (VI.4) we have plotted the theoretical expression for $P_{\uparrow}(h)$ for $\Delta=3$ along with the result of the corresponding simulation. The agreement is seen to be reasonably close.

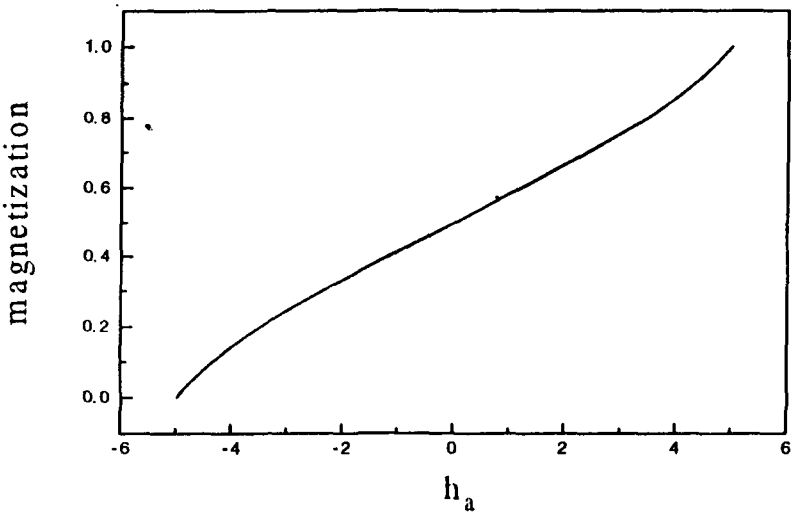

Fig.VI.4: Magnetization vs. applied field on the lower half of the hysteresis loop for $\Delta = 3|J|$.The simulation result is not distinguishable from the theoretical expression on the scale of the above figure.

CHAPTER–VII

VII. Summary and Concluding Remarks

The non-equilibrium response of complex physical systems shows a variety of interesting features. Computer simulations of minimal models have helped us in understanding several intricate aspects of non-equilibrium phenomena. There is also a need for simple, but exactly solved models that may provide a caricature of non-equilibrium phenomenology. The random field Ising model fits the bill adequately. Zero temperature Glauber dynamics of ferromagnetic RFIM describes systems that relax by avalanches. The non-equilibrium response of the ferromagnetic model has been obtained exactly in one dimension, and on a Bethe lattice. The distribution of avalanche sizes has been obtained as well, and has proved useful in explaining scale invariant aspects of the Barkhausen noise. Minor hysteresis loops have also been obtained. On the other hand, zero-temperature dynamics of anti-ferromagnetic RFIM describes systems that relax without avalanches. The work presented in this thesis is an attempt (perhaps the first attempt) to obtain the non-equilibrium response of the anti-ferromagnetic RFIM exactly. The problem, although very simple to state, appears unexpectedly difficult to us. We could only find an exact solution of the problem in one dimension in the case of a bounded rectangular distribution of the

random field of half-width $\Delta \leq |J|$, where $|J|$ is the strength of the anti-ferromagnetic interaction. We have also presented a solution for the case $\Delta > |J|$ but it is to be regarded as an approximate solution only, albeit very close to an exact solution. It is desirable to develop the techniques of statistical mechanics that would allow us to solve the problem stated here for an arbitrary, unbounded, continuous, distribution of the random field, and also to extend it in higher dimensions. We do not see a clear road to this end at the present time, but our efforts are likely to continue.

References

[1] See for example H.E. Stanley in: Introduction to phase transitions and critical phenomena, Clarendon Press, Oxford (1971).

[2] E. Ising, Z. Phys. **31**, 253, (1925).

[3] L.D. Landau and E.M. Lifschitz "Statistical Physics" 2nd edition, Pergamon Press Ltd., London (1969).

[4] N. Mermin and H. Wagner, Phys. Rev. Lett. **17**, 1133 (1966).

[5] L. Onsager, Phys. Rev. **65**, 117 (1944).

[6] C. Domb in : Phase Transitions and Critical Phenomena, eds. C. Domb and M.S. Green, Vol. **3**, Academic Press, London (1972).

[7] M. Wortis in : Phase Transitions and Critical Phenomena, eds. C. Domb and M.S. Green, Vol. **3**, Academic Press, London (1972).

[8] L.P. Kadanoff in: Phase Transitions and Critical Phenomena, eds.C. Domb and M.S. Green, Vol. **5A**, Academic Press, London (1976).

[9] K.G. Wilson, Phys. Rev. **B4**, 3174 (1971); 3184 (1971).

[10] K.G. Wilson and J.B. Kogut, Phys. Rep. **12C**, 75 (1974).

[11] K. Binder in : Phase Transition and Critical Phenomena, eds. C. Domb and M.S. Green, Vol. **5B**, Academic Press, London (1976).

[12] A.J. Bray, Lecture notes given in Summer College on Condensed Matter, ICTP (1997).

[13] A.J. Bray, Adv. Phys. **43**, 357 (1994); C.L. Emmott and A. J. Bray, Phys. Rev. **E54**, 4568 (1996); C.L. Emmott and A.J. Bray, Phys. Rev. **E59**, 213 (1999).

[14] D. Sherrington and S. Kirkpatrick, Phys. Rev. Lett. **5**, 1972 (1975).

[15] D. Chowdhury, Spin Glasses and Other Frustrated Systems, World Scientific, Singapore (1986).

[16] K. Binder and A.P. Young, Rev. Mod. Phys. **58**, 801 (1986).

[17] A.P. Young ed., Spin glasses and Random Fields, World Scientific, Singapore (1997).

[18] M. Mezard, G. Parisi and M.A. Virasoro, Spin Glass theory and beyond, World Scientific, Singapore (1987).

[19] J.J. Hopfield, Proc. Natl. Acad. Sci. USA, **79**, 2254 (1982); Ibid. **81**, 3088 (1984).

[20] D. Amit, Modelling Brain Function: The World of Attractor Neural Networks, Cambridge University Press, Cambridge (1989).

[21] D.J. Amit, H. Gutfreund, and H. Sompolinsky, Phys. Rev. Lett. 55, 1530 (1985); Ann. Phys. **173**, 30 (1987).

[22] P. Shukla, J. Stat. Phys. **71**, 705 (1993).

[23] P. Shukla and T.K. Sinha, Phys. Rev. **E47**, 2962 (1993).

[24] T.K. Sinha and P. Shukla, Phys. Rev. **E49**, R4811 (1994).

[25] P. Shukla, Phys. Rev. **E56**, 2265 (1997).

[26] S.N. Majumdar, Curr. Sci. (India) **77**, 370 (1999).

[27] G. I. Menon, P. Ray, P. Shukla, Phys. Rev. **E64**, 046102 (2001).

[28] L. Neel, J. Phys. et Rad. (Paris) **20**,215 (1959).

[29] J.S.W. Rayleigh, Phil. Mag. **23**, 225 (1887).

[30] F. Preisach, Z. Phys. 94, 277 (1935).

[31] M. Rao, H.R. Krishnamurthy, Rahul Pandit, Phys. Rev. **B42**, 856 (1990).

[32] D. Dhar and P.B. Thomas, J. Phys. A **25**, 4967 (1992); Europhys. Lett. **21**, 965 (1993).

[33] P.B. Thomas, Ph.D. thesis, TIFR/ Bombay University, 1993, and references therein.

[34] H. Barkhausen, Z. Phys. **20**, 401 (1919).

[35] P.J. Cote and L.V. Meisel, Phys. Rev. Lett. **67**, 1334 (1991); Phys. Rev. **B46**, 10822 (1992).

[36] G. Bertotti, G. Durin and A. Magni, J. Appl. Phys. **75**, 5490 (1994).

[37] D. Spasojevic, S. Bukvic, S. Milosevic and H.E. Stanley, Phys. Rev. **E54**, 2531 (1996).

[38] K.P.O' Brien and M.B. Weissman, Phys. Rev. **E50**, 3446 (1994) and references therein.

[39] B.K. Chakrabarti and M. Acharyya, Rev. Mod. Phys. **71**, 847 (1999); I.F. Lyuksyutov, T. Nattermann and V. Pokrovsky, Phys. Rev. **B59**, 4260 (1999).

[40] P. Bak, How Nature Works, Oxford University Press, Oxford (1997).

[41] D. Dhar, Phys. Rev. Lett. **67**, 1613 (1990).

[42] C.A. Angell and M. Goldstein (eds.), Annals of the New York Academy of Sciences, Vol. **484** (1986).

[43] J. Jackle, Rep. Prog. Phys. **49**, 171 (1986).

[44] A. Barrat, R. Burioni and M. Mezard, cond-mat/9509142.

[45] E.I. Shaknovich and A.M. Gutin, Europhys. Lett. **8**, 327 (1989); G. Iori, E. Marinari and G. Parisi, J. Phys. A **24**, 5439 (1991).

[46] G. Parisi, Order, Disorder and Simulations, World Scientific, Singapore (1992).

[47] Y. Imry and S.K. Ma, Phys. Rev. Lett. **35**, 1399 (1975).

[48] See for example, T. Nattermann, cond-mat 9705259.

[49] J.P. Sethna, K. Dahmen, S. Karta, J.A. Krumhansl, and J.D. Shore, Phys. Rev. Lett. **70**, 3347 (1993).

[50] P. Shukla, Physica A **233**, 235 (1996).

[51] D. Dhar, P. Shukla, and J. P. Sethna, J. Phys. A: Math. Gen. **30**, 5259 (1997).

[52] S. Sabhapandit, P. Shukla, and D. Dhar, J. Stat. Phys. **98**, 103 (2000).

[53] P. Shukla, Phys. Rev. **E62**, 4725 (2000).

[54] P. Shukla, Phys. Rev. **E63**, 027102 (2001).

[55] P. Shukla, Ind. J. Phys. **76A** (1), 51 (2002).

[56] S. Sabhapandit, D. Dhar, and P. Shukla, to appear in Phys. Rev. Lett. (2002).

[57] P. Shukla, Physica A **233**, 242 (1996).

[58] P. Shukla , Ind. J. Phys. **72A** (5), 439 (1998).

[59] P. Shukla, R. Roy, and Emilia Ray, Physica A **275**, 380 (2000).

[60] P. Shukla, R. Roy, and Emilia Ray, Physica A **276**, 365 (2000).

[61] J. Kisker , H. Rieger , H. Schreckenberg , J. Phys. A **27** L853 (1994). This paper discusses the non-equilibrium dynamics of a non-random, one-dimensional Ising model, with three-spin interactions, at low temperatures. It is qualitatively similar to the dynamics of the random field Ising model at zero-temperature.

[62] J. W. Evans , Rev. Mod Phys. **65**, 1281 (1993).

[63] L. G. Mityushin , Prob. Peredachi. Inf. **9**, 81 (1973).

Brief Bio-data of the Candidate

(as required by NEHU format for PhD thesis)

Ratnadeep Roy

"Destiny", Boyce Road,
Laitumkhrah,
Shillong- 793003 ;
phone: (0364)224164;
e-mail: ratnadeep@email.com

Born: February 27, 1971, Shillong; Single.

Academic Record:

High School	St. Peter's School	Shillong	1987
P.U.	St. Edmund's College	Shillong	1989
B.Sc	Shillong College	Shillong	1992
M.Sc	NEHU	Shillong	1995

Teaching Experience:

Taught Physics classes at Higher Secondary and Under-Graduate level at various colleges in Shillong.

Research Experience:

Work described in this thesis.

Other Interests:

History of Science, Computer hardware maintenance and networking.